



## Formation of highly oxygenated organic molecules from the oxidation of limonene by OH radical: significant contribution of H-abstraction pathway

Hao Luo<sup>1</sup>, Luc Vereecken<sup>2</sup>, Hongru Shen<sup>1</sup>, Sungah Kang<sup>2</sup>, Iida Pullinen<sup>2a</sup>, Mattias Hallquist<sup>3</sup>, Hendrik Fuchs<sup>2</sup>, Andreas Wahner<sup>2</sup>, Astrid Kiendler-Scharr<sup>2</sup>, Thomas F Mentel<sup>2\*</sup>, Defeng Zhao<sup>1,4,5,6\*</sup>

<sup>1</sup>Department of Atmospheric and Oceanic Sciences & Institute of Atmospheric Sciences, Fudan University, Shanghai, 200438, China

<sup>2</sup>Institute of Energy and Climate Research, IEK-8: Troposphere, Forschungszentrum Jülich, Jülich, 52425, Germany

<sup>3</sup>Department of Chemistry and Molecular biology, University of Gothenburg, Göteborg, 41258, Sweden

<sup>4</sup>Shanghai Frontiers Science Center of Atmosphere-Ocean Interaction, Fudan University, Shanghai 200438, China.

<sup>5</sup>Institute of Eco-Chongming (IEC), 20 Cuinia Rd., Chongming, Shanghai, 202162, China.

<sup>6</sup>CMA-FDU Joint Laboratory of Marine Meteorology, Fudan University, Shanghai 200438, China.

<sup>a</sup> Now at: Department of Applied Physics, University of Eastern Finland, Kuopio, 70210, Finland.

15 *Correspondence to:* Defeng Zhao (dfzhao@fudan.edu.cn), Thomas F Mentel (t.mentel@fz-juelich.de)

**Abstract.** Highly oxygenated organic molecules (HOM) play a pivotal role in the formation of secondary organic aerosol (SOA). Therefore, the distribution and yields of HOM are fundamental to understand their fate and chemical evolution in the atmosphere, and it is conducive to ultimately assess the impact of SOA on air quality and climate change. In this study, gas-phase HOM formed from the reaction of limonene with OH radical in photooxidation were investigated in the SAPHIR chamber (Simulation of Atmospheric PHotochemistry In a large Reaction chamber) using a time-of-flight chemical ionization mass spectrometer with nitrate reagent ion (NO<sub>3</sub>-CIMS). A large number of HOM, including monomers (C<sub>9-10</sub>) and dimers (C<sub>17-20</sub>), were detected and classified into various families. Both closed-shell products and open-shell peroxy radicals (RO<sub>2</sub>), were identified under low NO (0.1 ppt~0.2 ppb) and high NO conditions (17 ppb). C<sub>10</sub> monomers are the most abundant HOM products and account for over 80% total HOM. Closed-shell C<sub>10</sub> monomers were formed from two peroxy radical families, C<sub>10</sub>H<sub>15</sub>O<sub>x</sub>• (x=7-12) and C<sub>10</sub>H<sub>17</sub>O<sub>x</sub>• (x=8-13), and their respective termination reactions with NO, RO<sub>2</sub>, and HO<sub>2</sub>. While C<sub>10</sub>H<sub>17</sub>O<sub>x</sub>• is likely formed by OH addition to C<sub>10</sub>H<sub>16</sub>, the dominant initial step of limonene+OH, C<sub>10</sub>H<sub>15</sub>O<sub>x</sub>•, is likely formed via H-abstraction by OH. C<sub>10</sub>H<sub>15</sub>O<sub>x</sub>• and related products contributed 43% and 46% of C<sub>10</sub>-HOM at low and high NO, demonstrating that H-abstraction pathways play a significant role in HOM formation in the reaction of limonene+OH. Combining theoretical kinetic calculations, structure activity relationships (SARs), literature data, and the observed RO<sub>2</sub> intensities, we proposed tentative mechanisms of HOM formation from both pathways. We further estimated the molar yields of HOM to be 3.04<sup>+3.89</sup><sub>-1.64</sub>% and 0.82<sup>+1.05</sup><sub>-0.44</sub>% at low and high NO, respectively. Our study highlights the importance of H-abstraction by OH and provides yield and tentative pathways in the OH oxidation of limonene to simulate the HOM formation and assess their role in SOA formation.

### 1 Introduction

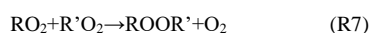
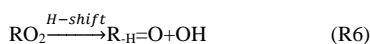
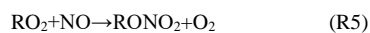
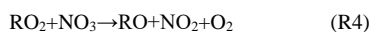
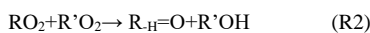
35 Biogenic volatile organic compounds (BVOC) are important precursors of atmospheric secondary organic aerosol particles (SOA) (Griffin et al., 1999; Kanakidou et al., 2005; Hallquist et al., 2009). In the Earth's atmosphere, monoterpenes (C<sub>10</sub>H<sub>16</sub>) are abundant BVOC with the second largest emission rate of approximately 150 Tg/year (Guenther et al., 2012). Among them, limonene accounts for 20% of total monoterpene emissions, ranking as the fourth largest (Guenther et al., 2012). In addition, as an important ingredient of essential oil and common volatile chemical product (VCP), limonene is also widely used in house  
40 cleaning and personal care products due to its pleasant fragrance and antimicrobial property. Hence, limonene can play an



important role in indoor SOA formation and indoor air quality (Waring, 2016; Rossignol et al., 2013; Nazaroff and Weschler, 2004). Although its concentration in the atmosphere is not the most abundant among monoterpenes, limonene has a high potential to form SOA due to its high SOA yield and high reactivity provided by the presence of an endocyclic and an exocyclic double-bond (Koch et al., 2000; Chen and Hopke, 2010; Gong et al., 2018; Saathoff et al., 2009).

- 45 Limonene can undergo gas-phase reactions rapidly with atmospheric oxidants such as the hydroxyl radical (OH) and ozone (O<sub>3</sub>) in daytime and the nitrate radical (NO<sub>3</sub>) and O<sub>3</sub> in nighttime forming peroxy radicals (RO<sub>2</sub>) (Lee et al., 2006b; Eddingsaas et al., 2012; Vereecken and Peeters, 2012; Zhang et al., 2018; Yu et al., 1999; Vereecken and Peeters, 2000). In the reaction of limonene with OH, the main atmospheric daytime loss process of limonene, OH addition to one of the olefinic carbon atoms is the dominant channel, although abstraction of an allylic hydrogen atom also occurs (Rio et al., 2010; Jokinen et al., 2014).
- 50 Via OH addition, the reaction forms C<sub>10</sub>H<sub>17</sub>O<sub>3</sub>• as a first-generation RO<sub>2</sub>, which under oxidative conditions further react with RO<sub>2</sub>, HO<sub>2</sub>, and NO forming oxidation products including limonaldehyde (C<sub>10</sub>H<sub>16</sub>O<sub>2</sub>), limonaketone (C<sub>9</sub>H<sub>14</sub>O), limonic acid (C<sub>10</sub>H<sub>16</sub>O<sub>3</sub>), ketolimononic acid (C<sub>9</sub>H<sub>14</sub>O<sub>4</sub>), peroxy-pinic acid or its isomer (C<sub>10</sub>H<sub>14</sub>O<sub>5</sub>), nitric acid ester (C<sub>9</sub>H<sub>13</sub>NO<sub>7</sub>), some organic acids with low molecular weight (formic acid, acetic acid, butyric acid, methacrylic), and formaldehyde (HCHO) (Pang et al., 2022; Friedman and Farmer, 2018; Romonosky et al., 2015; Jaoui et al., 2006; Lee et al., 2006a; Hakola et al.,
- 55 1994). Although earlier studies have gained valuable insights into the products and mechanism of the reaction with OH, many products and their formation mechanisms are not well elucidated. For example, highly oxygenated organic molecules (HOM) products and their formation mechanism remain elusive.

HOM was first discovered to be produced in forests and is defined as compounds containing six or more oxygen atoms formed in the gas phase via autoxidation (Bianchi et al., 2019; Ehn et al., 2012; Ehn et al., 2014). Among the myriad of oxygenated products, HOM was found of great importance for the mass of SOA, new particle formation and particle growth (Jokinen et al., 2015; Jokinen et al., 2014; Ehn et al., 2014; Mentel et al., 2015; Molteni et al., 2019; Kirkby et al., 2016; McFiggans et al., 2019; Crouse et al., 2013; Kenseth et al., 2018; Ehn et al., 2017; Krechmer et al., 2015; Quéléver et al., 2019; Tröstl et al., 2016). Typically, HOM are generated from the autoxidation of peroxy radicals (RO<sub>2</sub>), where a new, more oxygenated RO<sub>2</sub> can be formed after an intramolecular H-shift followed by O<sub>2</sub> addition in the resulting alkyl radical (Bianchi et al., 2019; Vereecken and Nozière, 2020; Crouse et al., 2013; Møller et al., 2019; Vereecken et al., 2007; Ehn et al., 2017; Nozière and Vereecken, 2019; Ehn et al., 2014). Biomolecular termination of the autoxidation chain occurs when an RO<sub>2</sub> intermediate react with HO<sub>2</sub>, RO<sub>2</sub>, and NO to form a series of products (see below), which can be classified as organic hydroperoxide (ROOH, R1), alcohol (ROH, R2), and carbonyl (R=O, R2), alkoxy radicals (RO, R3-4), or organic nitrates (ON, R5). The molecular masses of termination products are M+1, M-15, M-17 and M+30, respectively, for an RO<sub>2</sub> with molecular mass of M (Mentel et al., 2015; Ehn et al., 2014). Meanwhile, unimolecular termination pathways generally lead to the formation of carbonyls (R=O, R6). In addition, two RO<sub>2</sub> can also undergo an accretion reaction to form HOM dimers (R7) as the reactions shown below (Berndt et al., 2018; Valiev et al., 2019).



- 80 HOM formation in OH-initiated oxidation of monoterpenes such as  $\alpha$ -pinene and  $\beta$ -pinene has been studied in the laboratory (Berndt, 2021; Xu et al., 2019; Berndt et al., 2016; Kirkby et al., 2016; Ehn et al., 2014; Shen et al., 2022), and is assumed to mainly start with the OH addition to C=C double bond. The alkyl radical adduct can rapidly add O<sub>2</sub> to the radical site to form a peroxy radical (Finlayson-Pitts and Pitts, 2000; Ziemann and Atkinson, 2012). A number of monomers and dimers products



from several monoterpenes following the reaction with hydroxyl radical (OH) were observed, such as C<sub>10</sub>H<sub>14-16</sub>O<sub>7-11</sub> and C<sub>19-</sub>  
85 <sub>20</sub>H<sub>28-32</sub>O<sub>10-18</sub> (Berndt et al., 2018; Shen et al., 2022; Xu et al., 2019). Despite the molecular similarities of HOM monomers or  
dimers products from different monoterpenes (Jokinen et al., 2015; Ehn et al., 2014; Ehn et al., 2012), HOM yields are quite  
different between different monoterpenes in a given oxidation reaction (e.g. with O<sub>3</sub> or OH radical) (Jokinen et al., 2015). It  
follows that the HOM formation mechanisms for other monoterpenes may not necessarily be applicable to limonene. Although  
HOM formation from limonene by ozonolysis and NO<sub>3</sub> has been reported (Jokinen et al., 2015; Guo et al., 2022), to the best  
90 of our knowledge, no studies have systematically reported HOM distribution in limonene+OH. In the ozonolysis of limonene,  
Jokinen et al. (2014) attributed some HOM (C<sub>10</sub>H<sub>17</sub>O<sub>x</sub>•<sub>(x=5,7,9)</sub> (RO<sub>2</sub>)) to the reaction of limonene with OH produced in  
ozonolysis by comparing the mass spectra in the presence or absence of an OH scavenger. The composition and the formation  
mechanism of HOM in limonene photooxidation by OH remains unclear. Moreover, although the HOM yield of limonene+OH  
was determined, this yield was estimated based on the difference of the HOM yield in the ozonolysis with and without OH  
95 scavenger (Jokinen et al., 2015). It is necessary to confirm the yield by its direct determination in the reaction of limonene+OH.  
Interestingly, in our previous study, we found that hydrogen abstraction is important for HOM formation in the reaction of α-  
pinene+OH (Shen et al., 2022), where intermediate alkoxy radicals oxidation steps aid autoxidation by breaking the six-  
membered and four-membered rings. As limonene+OH is known to have a high H-abstraction contribution of ~34% (Rio et  
al., 2010; Dash and Rajakumar, 2015; Braure et al., 2014), it is interesting to compare these two systems due to the similar but  
100 subtly different structures of α-pinene and limonene, with both containing a six-membered ring whereas limonene does not  
contain a four-membered ring.

In this study, we investigated HOM from the photooxidation of limonene with OH at low NO (0.1 ppt~0.2 ppb) and high  
NO (17 ppb) in the SAPHIR chamber at Forschungszentrum Jülich. HOM were classified into monomers and dimers, and the  
product distribution is reported. The yields of HOM from limonene with OH were estimated. Formation mechanism of HOM  
105 in the OH reaction is proposed based on molecular formula of HOM and quantum chemical calculation as well as structure  
activity relationships (SARs) of RO<sub>2</sub> autoxidation rates. The relative importance of OH addition to C=C double bond and  
hydrogen abstraction by OH is discussed. We further investigated the effects of NO<sub>x</sub>, which changes HOM composition via  
altering the RO<sub>2</sub> fate.

## 2 Methodology

### 110 2.1 Experiment design and set-up

The experiments were conducted in the “SAPHIR” chamber (Simulation of Atmospheric PHotochemistry In a large Reaction  
chamber) at Forschungszentrum Jülich, Germany. The details of the chamber have been described in the previous studies  
(Zhao et al., 2018; Zhao et al., 2015b; Zhao et al., 2015a; Zhao et al., 2021; Rohrer et al., 2005; Shen et al., 2021; Guo et al.,  
2022). In brief, SAPHIR is a 270 m<sup>3</sup> Teflon chamber equipped with a louvre system to switch between natural sunlight for  
115 illumination and dark conditions. In this study, the experiments were conducted in sun light with the louvres opened.

Gas and particle phase species were characterized by a comprehensive set of instruments with the details described before  
(Zhao et al., 2015b). A Proton Transfer Reaction Time-of-Flight Mass Spectrometer (PTR-ToF-MS, Ionicon Analytik, Austria)  
was used for measuring VOC. A NO<sub>x</sub> analyzer (ECO PHYSICS TR480) and an UV photometer O<sub>3</sub> analyzer (ANSYCO, model  
O341M) were used to measure the concentrations of NO<sub>x</sub> and O<sub>3</sub>, respectively. A laser induced fluorescence system (LIF) was  
120 used to measure the concentrations of OH, HO<sub>2</sub> and RO<sub>2</sub> (Fuchs et al., 2012). A Scanning Mobility Particle Sizer Spectrometer  
(SMPS, TSI, DMA3081/CPC3785) was used to obtain particle number distributions. Temperature and relative humidity were  
continuously measured.

Before an experiment was conducted, the chamber was flushed with high purity synthetic air (purity>99.9999% N<sub>2</sub> and O<sub>2</sub>).  
Experiments were conducted at ~75% RH initially. In low NO condition, no NO was added and the background concentration



125 of NO, which mainly stems from HONO photolysis produced via a photolytic process from Teflon wall, is 0.1 ppt~0.2 ppb.  
At high NO condition, 17 ppb NO was added into the chamber first and limonene was sequentially added after half an hour.  
The louvres were opened ~40 min after adding limonene. To estimate the impact of ozone oxidation during photooxidation, we  
calculated the reaction rates of VOC+OH and VOC+O<sub>3</sub> in low and high NO conditions of this study (Fig. S1). During the first  
60 min, VOC+OH accounted for >99% limonene loss in both low and high NO condition. At low NO the RO<sub>2</sub> loss was  
130 estimated to be dominated by its reactions with NO in the early period (within ~2 h) and in later periods a significant fraction  
of RO<sub>2</sub> loss was also contributed by the reaction of RO<sub>2</sub> with HO<sub>2</sub> (Fig. S2), based on the measured NO<sub>x</sub>, RO<sub>2</sub>, and HO<sub>2</sub>  
concentrations and their rate constants for the reactions with RO<sub>2</sub> (Jenkin et al., 1997; Jenkin et al., 2019). At high NO, the  
RO<sub>2</sub> fate was by far dominated by the RO<sub>2</sub>+NO reaction.

## 2.2 Characterization of HOM

135 HOM were characterized by a Chemical Ionization time-of-flight Mass Spectrometer (CIMS, Aerodyne Research Inc., USA)  
with nitrate (<sup>15</sup>NO<sub>3</sub><sup>-</sup>) as the reagent ion, which has a mass resolution of ~4000 (m/dm). The details of the instrument are  
described in previous publications (Pullinen et al., 2020; Mentel et al., 2015; Ehn et al., 2014). Briefly, <sup>15</sup>NO<sub>3</sub><sup>-</sup> produced from  
<sup>15</sup>N nitric acid, was used as the reagent ion to distinguish complexation with the reagent ion from NO<sub>3</sub> groups in target  
molecules. NO<sub>3</sub><sup>-</sup>-CIMS is suitable for detecting oxygenated organic compounds with high oxygen number. The mass spectra  
140 were analysed by Tofware (version 2.5.7, Tofwerk/Aerodyne) in Igor Pro (version 6.37 WaveMetrics, Inc.). In this study, the  
mass spectra of HOM products during the first 60 min after louvres opening were analysed because the particle number  
concentration (<30 #/cm<sup>3</sup>) remained low in the initial phase of the reaction. After attributing molecular formulas of HOM to  
different m/z, their concentrations were calculated using the calibration coefficient of H<sub>2</sub>SO<sub>4</sub> (C: 2.5×10<sup>10</sup> molecule·cm<sup>-3</sup>·nc<sup>-1</sup>)  
as described before (Zhao et al., 2021; Pullinen et al., 2020), where the charge efficiency of HOM and H<sub>2</sub>SO<sub>4</sub> was assumed to  
145 be close to the collision limit (Pullinen et al., 2020; Ehn et al., 2014). The details of the calibration with H<sub>2</sub>SO<sub>4</sub> were described  
in Supplement Sect. S1. It is noted that the HOM yield is not very sensitive to the vapor wall loss rate, since HOM yields only  
change 11% to -6% upon an 100% increase and 50% decrease in wall loss rate (Zhao et al., 2021). The loss of HOM was  
corrected by using a wall loss rate of 2.2×10<sup>-3</sup> s<sup>-1</sup> in fan-on condition and ~6.0×10<sup>-4</sup> s<sup>-1</sup> in fan-off condition as quantified  
previously (Guo et al., 2022; Zhao et al., 2018), and a dilution loss rate ~1×10<sup>-6</sup> s<sup>-1</sup> (Zhao et al., 2015b). For details, we refer  
150 to these latter publications; briefly, the wall loss rate of HOM in our chamber was estimated as that of the decay of organic  
vapor concentrations in the dark. Overall, wall loss correction and dilution correction only affect the HOM yield by ~5.8% and  
<1%, respectively.

## 2.3 Data analysis

The HOM yield was obtained using the concentration of the HOM, divided by the concentration of limonene consumed by  
155 OH, which is the dominant oxidant of limonene and accounts for over 99% of limonene loss rate. HOM yield was calculated  
over the first 60 min after louvres opening as followed:

$$Y = \frac{\Delta[HOM]}{\Delta[VOC]_r} = \frac{I_{HOM} \cdot C}{\Delta[VOC]_r} \quad (\text{Eq. 1})$$

where  $\Delta[HOM]$  means the concentrations of total HOM corrected for wall loss and dilution loss,  $\Delta[VOC]_r$  is the consumption  
concentrations of limonene corrected for wall loss and dilution loss,  $I_{HOM}$  is the total signal intensity of HOM normalized to  
160 the total signal, and  $C$  is the calibration coefficient of H<sub>2</sub>SO<sub>4</sub>. The calibration and wall loss and dilution loss correction are  
described in detail in the Supplement (S1).

Based on the C<sub>10</sub> closed-shell products from unimolecular and bimolecular reactions of the C<sub>10</sub> peroxy radical families  
C<sub>10</sub>H<sub>15</sub>O<sub>x</sub>• and C<sub>10</sub>H<sub>17</sub>O<sub>x</sub>•, C<sub>10</sub>H<sub>16</sub>O<sub>x</sub> can be divided into carbonyls (R=O) and epoxides from C<sub>10</sub>H<sub>17</sub>O<sub>x</sub>•, as well as alcohols  
(ROH) and hydroperoxides (ROOH) from C<sub>10</sub>H<sub>15</sub>O<sub>x</sub>•. The contribution of C<sub>10</sub>H<sub>17</sub>O<sub>x</sub>•-related products to C<sub>10</sub>H<sub>16</sub>O<sub>x</sub>, was  
165 quantified as follows. For a HOM-RO<sub>2</sub>, the production rate of alcohols (ROH) can be obtained according to R2.



$$\frac{d[ROH]}{dt} = \alpha k_{RO_2+RO_2}[RO_2][RO_2]^T \quad (\text{Eq.2})$$

The production rate of hydroperoxides (ROOH) can be obtained according to R1.

$$\frac{d[ROOH]}{dt} = k_{RO_2+HO_2}[RO_2][HO_2] \quad (\text{Eq.3})$$

The production rate of carbonyls (R=O) can be obtained according to R2 and R6.

$$170 \quad \frac{d[R=O]}{dt} = (1 - \alpha)k_{RO_2+RO_2}[RO_2][RO_2]^T + k_{uni}[RO_2] \quad (\text{Eq.4})$$

Combing Eq.2-4, one can get Eq. 5:

$$\begin{aligned} \frac{\frac{d[ROH]}{dt} + \frac{d[ROOH]}{dt}}{\frac{d[R=O]}{dt}} &= \frac{\alpha k_{RO_2+RO_2}[RO_2][RO_2]^T + k_{RO_2+HO_2}[RO_2][HO_2]}{(1 - \alpha)k_{RO_2+RO_2}[RO_2][RO_2]^T + k_{uni}[RO_2]} \\ &= \frac{\alpha k_{RO_2+RO_2}[RO_2]^T + k_{RO_2+HO_2}[HO_2]}{(1 - \alpha)k_{RO_2+RO_2}[RO_2]^T + k_{uni}} \end{aligned} \quad (\text{Eq. 5})$$

where  $[RO_2]^T$  and  $[HO_2]$  are the total concentrations of  $RO_2$  and the concentration of  $HO_2$  in the reaction system, respectively.

175  $k_{uni}$ ,  $k_{RO_2+RO_2}$  and  $k_{RO_2+HO_2}$  represent the rate coefficient of the unimolecular termination of  $RO_2$  and the bimolecular reactions of  $RO_2$  with  $RO_2$  and  $HO_2$ .  $\alpha$  and  $1-\alpha$  are the carbonyl yield and the alcohol yield in reactions of  $RO_2 + RO_2$ , respectively. As shown in the Eq. 2, we assume the same  $k_{uni}$ ,  $k_{RO_2+RO_2}$ ,  $k_{RO_2+HO_2}$ , and  $\alpha$  for a given  $C_{10}H_{15}O_x$  and  $C_{10}H_{17}O_x$  family. Wall loss was neglected due to its minor effects on the concentrations of the products (~5.8%).

For  $C_{10}H_{15}O_x$  family, the Eq. 5 is equivalent to Eq. 6:

$$180 \quad \frac{d[C_{10}H_{16}O_x]_{ROH+ROOH}}{d[C_{10}H_{14}O_x]} = \frac{d[C_{10}H_{16}O_x] \times (1-[R=O]\%)}{d[C_{10}H_{14}O_x]} \quad (\text{Eq. 6})$$

For  $C_{10}H_{17}O_x$  family, the Eq. 5 is equivalent to Eq. 7:

$$\frac{d[C_{10}H_{18}O_x]}{d[C_{10}H_{16}O_x]_{R=O}} = \frac{d[C_{10}H_{18}O_x]}{d[C_{10}H_{16}O_x] \times [R=O]\%} \quad (\text{Eq. 7})$$

Consequently, the ratios of  $\frac{d[ROH]+d[ROOH]}{d[R=O]}$  for  $C_{10}H_{15}O_x$  and  $C_{10}H_{17}O_x$  are the same. Eq. 8 can then be derived from Eq. 3 and 4, to yield  $[R=O]\%$ , which represents the contribution of the carbonyls produced from  $C_{10}H_{17}O_x$  to  $C_{10}H_{16}O_x$ .

$$185 \quad \frac{d[C_{10}H_{16}O_x] \times (1-[R=O]\%)}{d[C_{10}H_{14}O_x]} = \frac{d[C_{10}H_{18}O_x]}{d[C_{10}H_{16}O_x] \times [R=O]\%} \quad (\text{Eq. 8})$$

Based on this, about 92% and 97% of  $C_{10}H_{16}O_x$  were estimated to be carbonyls from  $C_{10}H_{17}O_x$  at low and high  $NO$ , respectively.

## 2.4 Theoretical kinetic study of $C_{10}H_{15}O$ alkoxy and $C_{10}H_{15}O_2$ peroxy radicals

The formation mechanism of  $C_{10}H_{15}O$  alkoxy and  $C_{10}H_{15}O_2$  peroxy radicals were considered in the theoretical kinetic study.

190 The geometries of the intermediates and transition states for the first steps in the mechanism were first optimized using the M06-2X/cc-pVDZ methodology (Zhao and Truhlar, 2008; Dunning, 1989), with an exhaustive characterization of all conformers for each reactant and transition state. All geometries obtained thus were further optimized at the M06-2X-D3/aug-cc-pVTZ level of theory which includes D3 diffusion corrections (Goerigk et al., 2017; Grimme et al., 2011). Moments of inertia for molecular rotation, and wavenumbers for vibration were obtained at the same level of theory, with a vibrational scaling factor of 0.971 (Alecú et al., 2010; Dunning, 1989). The barrier heights were further improved by single-point calculations at the CCSD(T)/aug-cc-pVTZ level of theory (Dunning et al., 2001; Bartlett and Purvis, 1978) (all T1 diagnostics  $\leq 0.029$ ). The expected uncertainty on the reaction barrier heights at this level of theory is  $\pm 0.5$  kcal mol<sup>-1</sup>. All quantum chemical calculations were performed using the Gaussian-16 software suite (Frisch et al., 2016). The quantum chemical data underlying the theoretical kinetic calculations is provided in the supplement.

200 The rate coefficients for the individual reactions at the high-pressure limit were then calculated using multi-conformer transition state theory, MC-TST (Vereecken and Peeters, 2003), incorporating the data for all conformers obtained as described above. Tunnelling is accounted for using an asymmetric Eckart barrier correction (Johnston and Heicklen, 1962; Eckart, 1930).



Based on earlier work at a similar level of theory in comparison with experimental data on H-migration in RO<sub>2</sub>• radicals with no or only one oxygenated functionality (Vereecken and Nozière, 2020; Nozière and Vereecken, 2019) and available  
205 theoretical literature data on ring closure reactions (Vereecken et al., 2021), we estimate the thermal rates to be accurate to a factor 2 to 3.

## 2.5 SAR-based mechanism development for autoxidation

The kinetics of the chemistry following the ring breaking is expected to be fairly well described based on structure-activity relationships (SARs), and no explicit theoretical kinetic calculations were performed. We employ the same approach for  
210 deducing the mechanism as described in our recent work (Shen et al., 2022). Briefly, we only consider a limited oxidation network by considering all possible reaction channels, predict their rate by SARs, and select few dominant channels. For the rate coefficients for most H-migrations in RO<sub>2</sub>• radicals, we base ourselves on the SAR by Vereecken and Nozière (2020); this SAR was reported to reproduce the scarce experimental data within a factor of 2, but for multi-functionalized species such as  
215 cycloperoxides, we additionally rely on the systematic study by Vereecken et al. (2021), who explicitly calculated rate coefficients for peroxy radicals formed after RO<sub>2</sub>• ring closure reactions. For those reaction classes that are not covered by either SAR, we estimate a rate by extrapolating the reactivity trends in the SARs, albeit with a large uncertainty. For ring closure reactions in unsaturated RO<sub>2</sub>• we employ on the SAR by Vereecken et al. (2021), where it is assumed that the presence of another cycloperoxide ring does not influence the rate. In assessing the fate of an RO<sub>2</sub>• radical with one or more -OOH  
220 groups, we account for the possibility of H-atom scrambling, as described extensively in the literature (Praske et al., 2019; Møller et al., 2019; Jørgensen et al., 2016; Nozière and Vereecken, 2019; Knap and Jørgensen, 2017). These fast H-migrations between the -OO• and -OOH groups are typically much faster than other unimolecular channels, leading to a fast equilibration among all accessible OOH-substituted RO<sub>2</sub>• radicals, and the dominant reaction is chosen among those available to the pool of RO<sub>2</sub>• radicals. We refer to Vereecken and Nozière (2020) for a more detailed description of this feature. In the early stages  
225 of the oxidation, we also use the recent work by Piletic and Kleindienst (2022). Finally, for alkoxy radical chemistry, we employ the SARs for decomposition and H-migration by Novelli et al. (2021) and Vereecken and Peeters (2009, 2010). For hydroperoxyl-substituted alkoxy radicals we note explicitly that H-migration of the hydroperoxide H-atom, forming an alcohol and an RO<sub>2</sub> radical, is typically very fast,  $k(298\text{ K}) \geq 10^{10}\text{ s}^{-1}$  (Vereecken and Nozière, 2020), and is often the most likely loss process in later alkoxy stages in the autoxidation chain. This fast H-migration supports competitive autoxidation even under  
230 high-NO conditions despite the formation of alkoxy intermediates that threaten to fragment the molecule.

## 3 Results and discussion

### 3.1 Overview of HOM spectra

The mass spectra of gas phase products HOM formed in the oxidation of limonene by OH at two different NO<sub>x</sub> levels are demonstrated in the Fig. 1. The HOM products can be classified according their mass to charge ratio (m/z) as either monomers  
235 (200-400 Th, including C<sub>6</sub>-C<sub>9</sub> monomers and C<sub>10</sub> monomers (320-400 Th)) or dimers (480-600 Th, C<sub>17</sub>-C<sub>20</sub> dimers). We did not observe any trimer products. The signal intensity of monomers is higher than dimers at both low and high NO (Fig. 1 and Fig. 2), where monomers accounted for over 80% of total HOM. Both the signal intensity and the fraction of the observed dimers at high NO were much less than that at low NO (Fig. 1 and Fig. 2). In the following (Sect. 3.2) we discussed product distribution and formation mechanism of monomers and dimers in details.

240

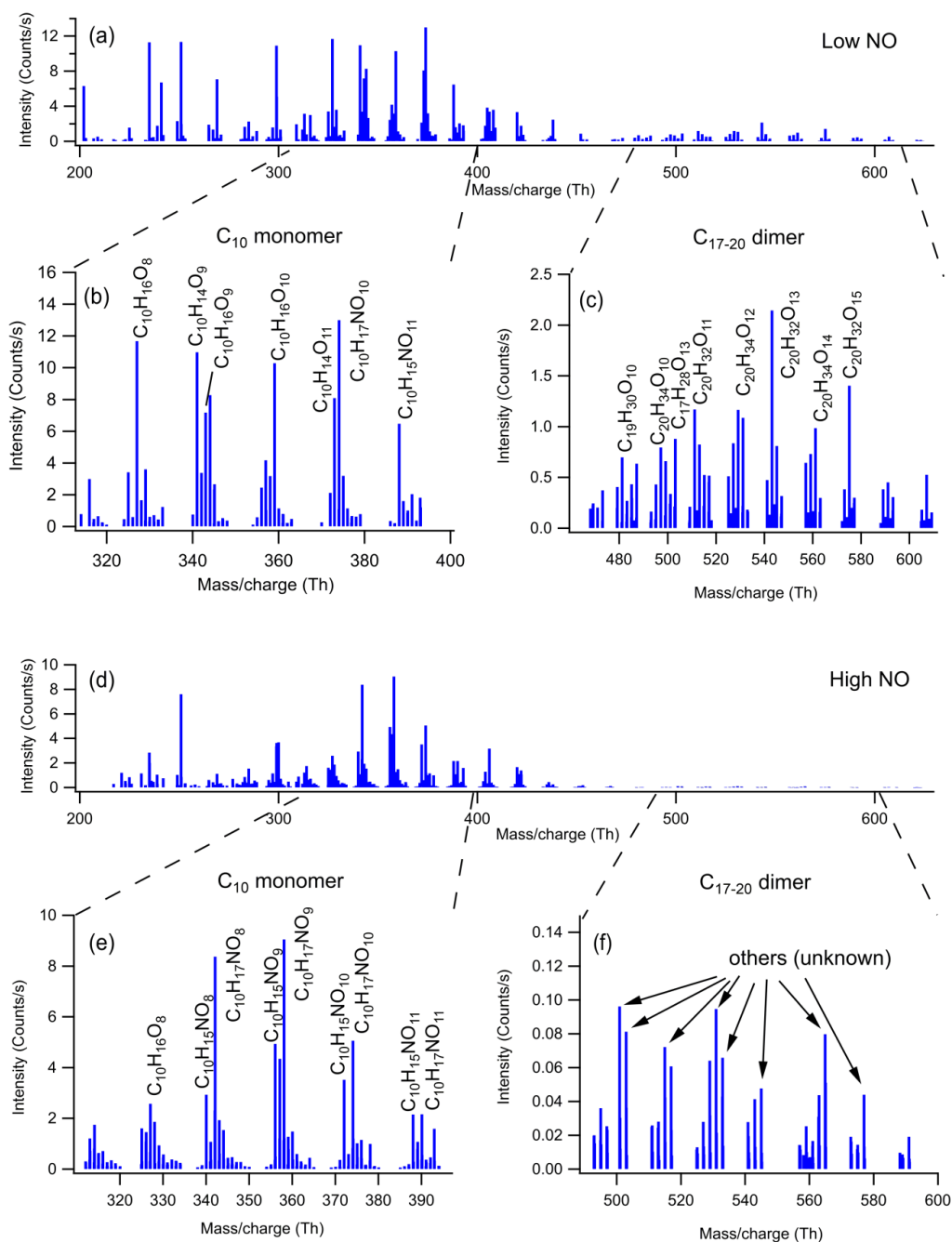


**Figure 1.** Mass spectrum of the HOM formed in the oxidation of limonene by OH in (a) low and (d) high NO condition. The mass spectra were obtained within 60 min after opening the louvres and were averaged over 60 min. Figure 1 (b, c, e, f) present expanded mass spectra where major peaks are labelled with their molecular formula.

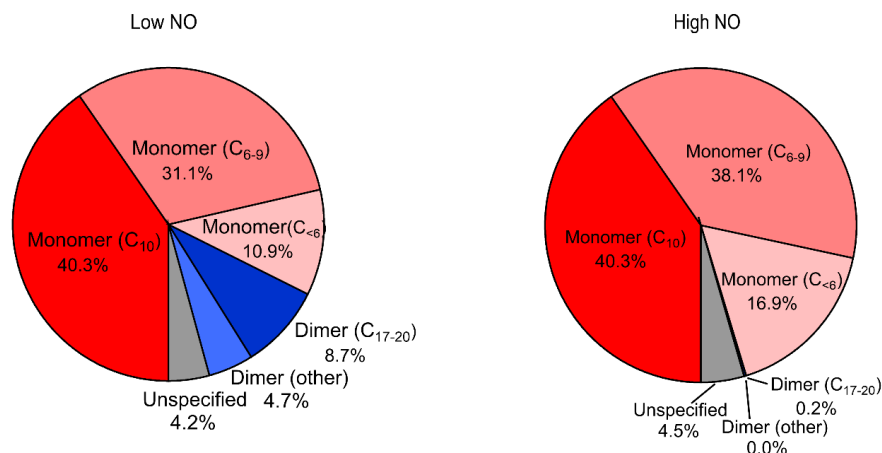


**Figure 2.** HOM product distribution including monomers (C<sub>10</sub>, C<sub>6-9</sub>, C<sub><6</sub>), dimers (C<sub>17-20</sub>, other), and unspecified species in low and high NO conditions.

## 250 3.2 Identification and formation mechanism of HOM

### 3.2.1 Overview of HOM monomers

Closed-shell HOM monomers are characterized by repeating pattern of molecular formulas with an increasing number of oxygen atoms in the mass spectrum. The repeating pattern in the mass spectrum at every 16 Th form series of HOM monomer families, such as C<sub>6</sub>H<sub>8/10</sub>O<sub>x</sub>, C<sub>6</sub>H<sub>9/11</sub>NO<sub>x</sub>, C<sub>7</sub>H<sub>8/10/12</sub>O<sub>x</sub>, C<sub>7</sub>H<sub>9/11</sub>NO<sub>x</sub>, C<sub>8</sub>H<sub>10/12/14</sub>O<sub>x</sub>, C<sub>8</sub>H<sub>11/13</sub>NO<sub>x</sub>, C<sub>9</sub>H<sub>12/14/16</sub>O<sub>x</sub>, C<sub>9</sub>H<sub>13/15</sub>NO<sub>x</sub>,  
255 C<sub>10</sub>H<sub>14/16/18</sub>O<sub>x</sub>, and C<sub>10</sub>H<sub>15/17</sub>NO<sub>x</sub> (Fig. S3). It is worth noting that some open-shell radicals, such as C<sub>10</sub>H<sub>15</sub>O<sub>x</sub>•(x=7-12) and C<sub>10</sub>H<sub>17</sub>O<sub>x</sub>•(x=8-13), were also observed; these are a significant fraction of HOM monomers and will be discussed in detail in section 3.2.2. These open-shell molecules were likely RO<sub>2</sub> radicals, as we are not able to detect the very short lived alkoxy radicals (RO) and alkyl radicals (R). The closed shell products (C<sub>≤10</sub>H<sub>y</sub>O<sub>x</sub> and C<sub>≤10</sub>H<sub>y</sub>NO<sub>x</sub>) will be discussed in the following from the perspective of RO<sub>2</sub> chemistry, i.e. as termination products of RO<sub>2</sub>. It should be noted that each molecular mass can  
260 represent several isomers, and that there may be more than one pathway to form a given product; our experiments do not allow to discriminate these and an in-depth discussion is outside the scope of this work.

HOM monomers were classified into C<sub>10</sub> and C<sub>6-9</sub> monomers according to the numbers of carbon atoms. The abundance of C<sub>6-9</sub> monomers (~30 % combined) was lower than C<sub>10</sub> compounds (~40 %) at low NO. In addition to C<sub>10</sub> and C<sub>6-9</sub> monomers, other monomers accounted for ~25% of all monomers and unspecified monomers accounted for ~5%. As shown in Fig. S3,  
265 C<sub>6-10</sub> monomers contain either none or one nitrogen atoms, and a higher fraction of organic nitrates was observed in high NO condition (nitrate HOM: 33% at low NO and 45% at high NO). This is as expected given that the fraction of RO<sub>2</sub> terminated by NO forming organic nitrate was higher at high NO. Higher fractions of organic nitrate have also been observed by the previous studies in the photo-oxidation of other monoterpenes at high NO (Pullinen et al., 2020; Shen et al., 2022).

### 3.2.2 C<sub>10</sub> monomer product distribution

270 At both low and high NO condition, C<sub>10</sub> compounds (C<sub>10</sub>H<sub>14</sub>O<sub>x</sub>, C<sub>10</sub>H<sub>15</sub>NO<sub>x</sub>, C<sub>10</sub>H<sub>16</sub>O<sub>x</sub>, C<sub>10</sub>H<sub>17</sub>NO<sub>x</sub> and C<sub>10</sub>H<sub>18</sub>O<sub>x</sub>) were the most abundant monomers with a fractional contribution of ~40% (see Fig. 2). In this study, we observed two major RO<sub>2</sub> radical families, C<sub>10</sub>H<sub>15</sub>O<sub>x</sub>•(x=7-12) and C<sub>10</sub>H<sub>17</sub>O<sub>x</sub>•(x=8-13), and their corresponding termination products, C<sub>10</sub>H<sub>14</sub>O<sub>x-1</sub>, C<sub>10</sub>H<sub>16</sub>O<sub>x-1</sub>, C<sub>10</sub>H<sub>16</sub>O<sub>x</sub>, and C<sub>10</sub>H<sub>15</sub>NO<sub>x+1</sub>, and C<sub>10</sub>H<sub>16</sub>O<sub>x-1</sub>, C<sub>10</sub>H<sub>18</sub>O<sub>x-1</sub>, C<sub>10</sub>H<sub>18</sub>O<sub>x</sub>, and C<sub>10</sub>H<sub>17</sub>NO<sub>x+1</sub> respectively, which contained carbonyl, hydroxyl, hydroperoxyl and nitrate, respectively (see Fig. 3, Table S1, Table S2, Table S5, and Table S6). C<sub>10</sub>H<sub>14</sub>O<sub>x</sub> and



275  $C_{10}H_{16}O_x$  were likely carbonyl compounds formed via unimolecular termination of  $C_{10}H_{15}O_x^\bullet$  and  $C_{10}H_{17}O_x^\bullet$ , respectively. Overall, at high NO, organic nitrates were the most abundant among all classes of HOM monomers and their relative proportion was much higher than at low NO (Fig. 3). Under low NO condition,  $C_{10}H_{14}O_x$  and  $C_{10}H_{16}O_x$  family are the two most abundant family among  $C_{10}$  monomers. This is similar to the  $C_{10}$  monomers products from photooxidation of  $\alpha$ -pinene by OH radical (Shen et al., 2022).

280

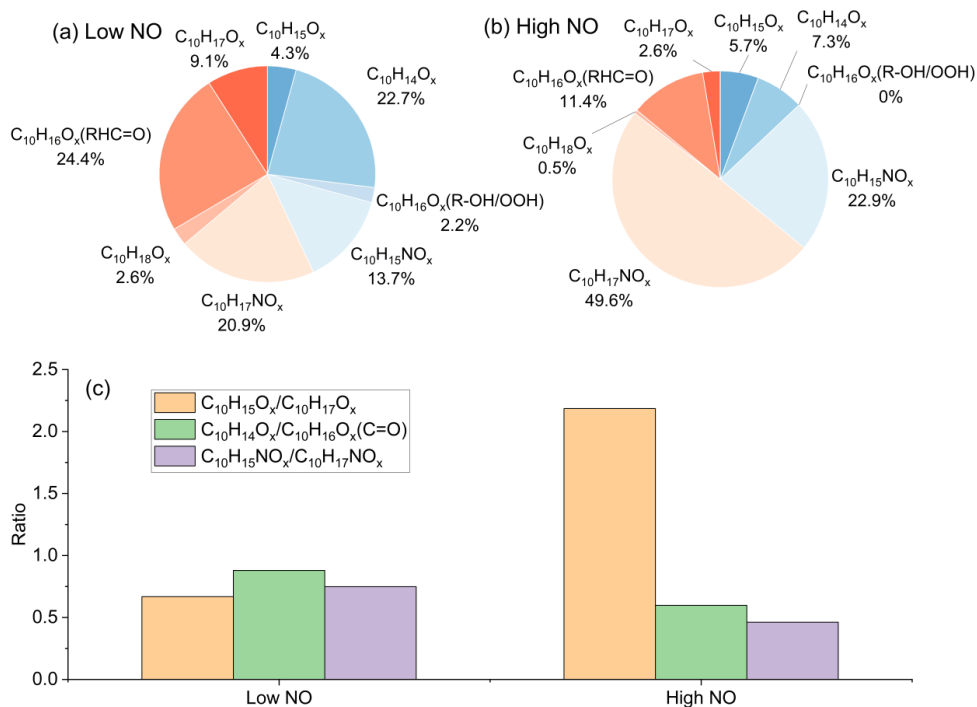


**Figure 3.** Product distribution within  $C_{10}$  monomers at low (a) and high NO (b) and the ratio of  $C_{10}H_{15}O_x^\bullet$  to  $C_{10}H_{17}O_x^\bullet$  and of their termination products (c). As in Fig.2, data of the first 60 min of the experiments were used.



### 285 3.2.3 Monomers with $C_{<10}$ monomers and dimers

A number of monomers with carbon number less than 10 ( $C_{<10}$ ) were observed in this study. The monomers ( $C_{<10}$ ) account for about 30% of the total monomers. The two radicals  $C_7H_9O_x^\bullet$  and  $C_7H_{11}O_x^\bullet$  were likely produced from  $C_{10}H_{15}O_x^\bullet$  radicals and  $C_{10}H_{17}O_x^\bullet$  radicals, respectively (see below). The ratios of total termination products from  $C_7H_9O_x^\bullet$  to those from  $C_7H_{11}O_x^\bullet$  are 1.8 and 1.2 at low and high NO respectively, which is generally consistent with the ratio of  $C_{10}H_{15}O_x^\bullet$  radicals and

290  $C_{10}H_{17}O_x^\bullet$  radicals for  $C_{10}$ -related products. This suggests that chemistry related to  $C_{10}H_{15}O_x^\bullet$  radicals plays a significant role in formation of  $C_{<10}$  monomers. Although the concentrations of monomers ( $C_{<10}$ ) are smaller than of  $C_{10}$  monomers, they may also contribute to the formation of dimers, which further condense onto particles.

We observed a number of dimer families, including  $C_{20}H_{30}O_x$  ( $x=10,12-18$ ),  $C_{20}H_{32}O_x$  ( $x=9-18$ ),  $C_{20}H_{34}O_x$  ( $x=10-17$ ),  $C_{19}H_{32}O_x$  ( $x=10-15$ ),  $C_{19}H_{31}NO_x$  ( $x=11-18$ ),  $C_{19}H_{30}O_x$  ( $x=10-17$ ),  $C_{18}H_{30}O_x$  ( $x=10-14$ ),  $C_{19}H_{28}O_x$  ( $x=11-15$ ),  $C_{17}H_{26}O_x$  ( $x=11-15$ ),  $C_{17}H_{24}O_x$  ( $x=12-17$ ) in low NO condition, and  $C_{20}H_{30}O_x$  ( $x=12-16$ ),  $C_{20}H_{32}O_x$  ( $x=11-18$ ),  $C_{20}H_{34}O_x$  ( $x=10-15$ ),  $C_{19}H_{28}O_x$  ( $x=11-17$ ),  $C_{17}H_{26}O_x$  ( $x=12-15$ ) in high NO condition (see Table S3 and Table S4). Compared to monomers, the peak intensity of dimers both at low and high NO conditions are much lower (Fig. S4 and Fig. S5). Furthermore, the peak intensity of dimers in low NO condition is higher than that in high NO condition. This inhibitory effect of  $NO_x$  in dimer formation is consistent with the phenomenon described in previous studies (Pullinen et al., 2020; Yan et al., 2016; Shen et al., 2022). In the following

300 discussion we will focus on  $C_{10}$  monomers. However, more information on  $C_{<10}$  monomers and dimers can be found in Supplement Sect. S2.

### 3.3 Formation pathways of HOM monomers

In this section we discuss potential formation pathways for  $C_{10}$  monomers. These pathways are tentative only, and are based on the current knowledge on autoxidation as represented in various SARs, where we examine only those paths estimated as

305 being the fastest. Our observations do not distinguish between different isomers and we cannot validate the reaction scheme. We also observed HOM with only 7, 8 or 9 carbon atoms and their possible formation pathways, involving a fragmentation step in an intermediate alkoxy radical, are inspected in the supporting information (see schemes S1 and S2).

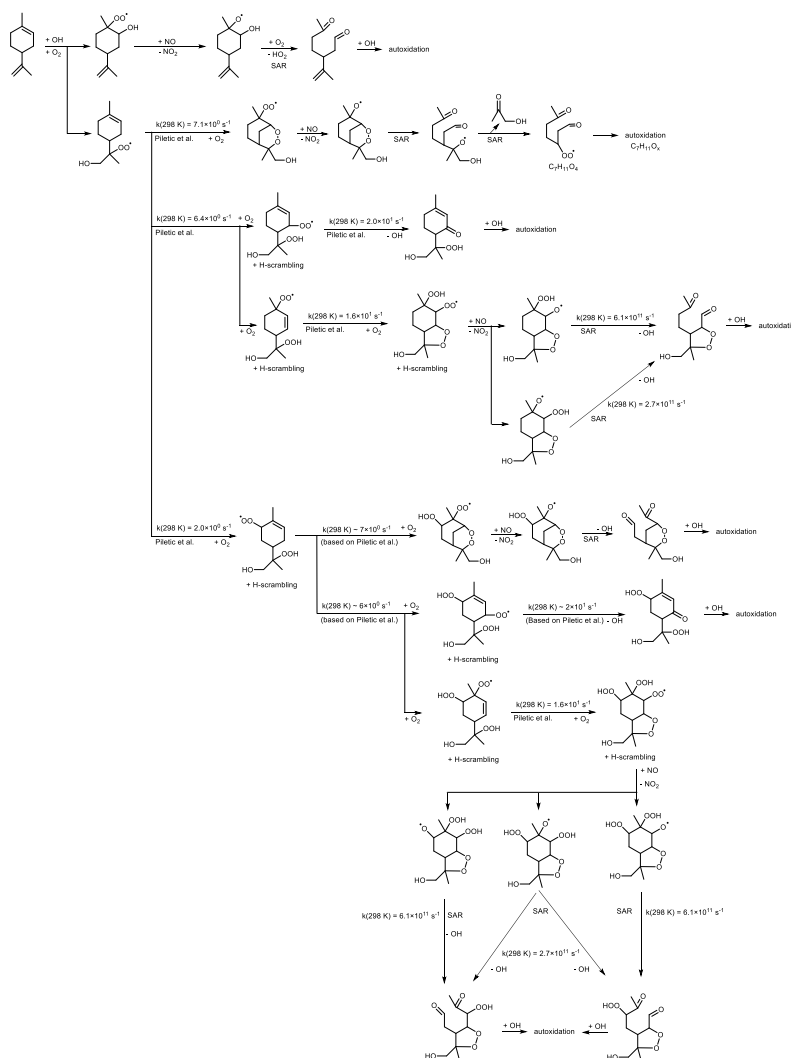
#### 3.3.1 HOM from OH addition

The  $C_{10}H_{17}O_x^\bullet$  radicals are formed from the OH addition reaction of limonene and subsequent autoxidation (see Table S2). Scheme 1 shows possible oxidation routes for the OH addition to both double bonds, considering the particular channels leading to tertiary alkyl radicals and depicting the most likely reactions as estimated based on theoretical work and SARs (Peeters et al., 1999; Vereecken et al., 2007; Jenkin et al., 2018). The  $C_{10}H_{17}O_3^\bullet$   $RO_2$  radical formed after  $O_2$  addition on the OH adducts has access to a wide range of reactions, but in most cases the six-membered ring is retained in the first  $RO_2$  steps, leading to slow autoxidation steps (Vereecken et al. 2021). This allows the reaction with NO to become important, whereafter

315 the decomposition of a  $\beta$ -OH or  $\beta$ -OOH alkoxy radical leads to carbonyl formation and thus chain termination. This analysis suggests that HOM formation after OH addition either proceeds through less favourable pathways or involves secondary chemistry. The complete explicit mechanism is highly branched and complex, and missing pathways in Scheme 1 could together contribute to sizable HOM formation. Furthermore, the rate estimates are tentative, with uncertainties of an order of magnitude or more, so we cannot exclude that primary HOM formation is possible and important. The primary products

320 predicted in Scheme 1 (or formed through similar termination reactions in other channels) can react again with OH, initiating secondary autoxidation. Most of these products have the six-membered ring broken, and should be more amenable to further autoxidation steps and thus readily yield HOM. However, this extra bimolecular OH reaction takes time, and can delay formation of HOM. An analysis of the secondary chemistry is outside the scope of this work, and at this time we do not propose a reaction scheme that covers the full range of  $C_{10}H_{17}O_x^\bullet$  radicals and related products observed.

325 In our previous study, the average bimolecular RO<sub>2</sub> loss rate was estimated at ~0.02 s<sup>-1</sup> (low NO) and ~3.5 s<sup>-1</sup> (high NO) (Zhao et al., 2018). In both cases RO<sub>2</sub> loss is due predominantly to the reaction with NO (see Figure S2), which leads to the organic nitrate termination products, as illustrated in Fig. 3. Even at low NO with ~0.2 ppb, organic nitrates (C<sub>10</sub>H<sub>15</sub>NO<sub>x</sub> and C<sub>10</sub>H<sub>17</sub>NO<sub>x</sub>) contribute a large portion of HOM (29%). The relevant termination products from C<sub>10</sub>H<sub>17</sub>O<sub>x</sub>• (x=8-13) in reactions with HO<sub>2</sub> and RO<sub>2</sub> are identified as C<sub>10</sub>H<sub>18</sub>O<sub>x</sub>, C<sub>10</sub>H<sub>18</sub>O<sub>x-1</sub>, and C<sub>10</sub>H<sub>16</sub>O<sub>x-1</sub>. However, C<sub>10</sub>H<sub>18</sub>O<sub>x</sub> accounted for only 2.6% and 330 0.5% in C<sub>10</sub> monomers at low and high NO, respectively, as in high NO conditions these loss processes are overwhelmed by the RO<sub>2</sub> + NO reaction.



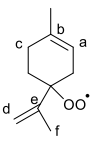
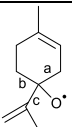
**Scheme 1.** Example reaction scheme for C<sub>10</sub>H<sub>17</sub>O<sub>x</sub>• RO<sub>2</sub> formation after OH-addition in limonene, based on the most likely reactions predicted in theoretical work and SAR predictions. All RO<sub>2</sub> intermediates have competing reactions (not shown) under current conditions with HO<sub>2</sub> (forming hydroperoxides) and NO (forming alkoxy and nitrates).

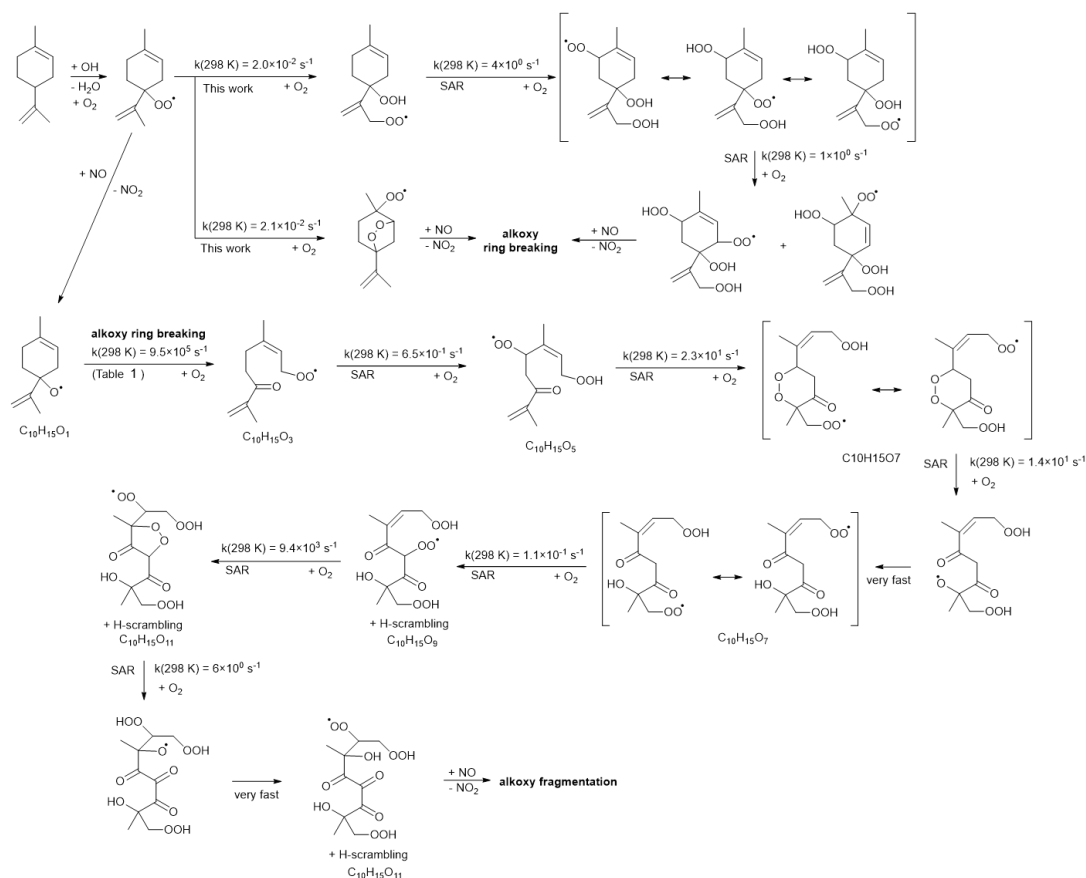


### 3.3.2 HOM from H-abstraction by OH

The observed  $C_{10}H_{15}O_x^\bullet$  radicals can only originate from an H-abstraction reaction by OH, removing one of the limonene H-atoms. An example pathway for  $C_{10}H_{15}O_x^\bullet \cdot RO_2$  radical formation is shown in Scheme 2, based on the most facile H-abstraction channel from limonene. The nascent peroxy radical formed after H-abstraction of the allylic tertiary H-atom in limonene is not amenable to efficient autoxidation and HOM formation, due to the geometric constraints in the ring. Theoretical kinetic calculations (see Table 1) show that the fastest autoxidation steps occur at rates of  $\sim 2 \times 10^{-2} \text{ s}^{-1}$ , i.e. of similar magnitude as the  $RO_2$  loss with NO in the low-NO experiments, but negligible against the  $RO_2 + NO$  rate at high NO. Our rate predictions agree with the recent theoretical study by Piletic and Kleindienst (2022). Further autoxidation steps with the ring structure intact are expected to be unfavourable, as well as autoxidation initiated through other H-abstraction sites (Vereecken et al., 2021; Piletic and Kleindienst, 2022). The reaction of the primary  $RO_2$  with NO, however, leads to an alkoxy radical that is most likely to break the six-membered ring, with a total rate coefficient exceeding  $\sim 10^6 \text{ s}^{-1}$  (see Table 1). This alkoxy-peroxy autoxidation step thus removes the geometric constraint, and fast autoxidation reactions become accessible, with rates enhanced by the presence of the double bonds (Vereecken and Nozière, 2020; Møller et al., 2019). Each of these autoxidation steps needs to compete against bimolecular reactions with NO, suggesting that more alkoxy-peroxy steps are likely. Some of these alkoxy intermediates will preferentially break the carbon backbone, leading to fragmentation, while other alkoxy radicals will proceed by H-migration and continue the autoxidation chain. In the latter case, autoxidation then no longer follows the systematic series of adding 2 O-atoms per autoxidation step, and the  $C_{10}H_{15}O_x^\bullet$  formation mechanism can proceed both by even-numbered and odd-numbered oxygen numbers  $x$ . At high NO concentrations, formation of alkoxy radicals becomes more likely, and thus fragmentation can become more prominent, reducing the yield of  $C_{10}H_{15}O_x^\bullet$  related HOM. This is in agreement with the current observations, where more fragment  $C_{<10}$  monomers (57.7% in total monomers) are observed at high NO, than at low NO (51.0 %). Further autoxidation of the fragments is also possible, leading to  $C_{<10}$  monomers and dimer formation, as discussed in the supplement.

**Table 1.** H-migration, ring closure and C-C bond scission reactions in  $RO_2^\bullet$  and  $RO^\bullet$  radicals formed from limonene H-abstraction, listing barrier heights  $E_b$  (kcal mol $^{-1}$ ), rate coefficient  $k$  at 298 K ( $\text{s}^{-1}$ ), and parameters for a Kooij equation fit  $k(T) = A \times T^n \times \exp(-E_a/T)$  for the temperature range 200–450 K, calculated using the CCSD(T)/M06-2X-D3 level of theory.

$RO_2^\bullet$	Reaction type	$E_b$	$k(298\text{K})$	$A / \text{s}^{-1}$	$n$	$E_a / \text{K}$
	5-Ring closure (a)	19.0	$2.1 \times 10^{-2}$	5.40E+07	1.40	8840
	6-Ring closure (b)	20.2	$1.8 \times 10^{-3}$	6.35E+07	1.27	9390
	Allyl-1,5-H-shift (c)	24.4	$1.2 \times 10^{-3}$	6.45E-91	32.94	-3977
	4-Ring closure (d)	26.9	$2.4 \times 10^{-8}$	2.50E+03	2.79	12292
	5-Ring closure (e)	29.8	$2.3 \times 10^{-10}$	1.04E+03	2.83	13489
	Allyl-1,5-H-shift (f)	22.5	$2.0 \times 10^{-2}$	8.68E-81	29.51	-3667
Other H-migrations lead to high ring strain and are not competitive						
	Ring opening (a)	9.4	$9.5 \times 10^5$	7.60E+08	1.42	4409
	Ring opening (b)	10.5	$1.6 \times 10^5$	1.01E+09	1.39	4972
	Fragmentation (c)	17.4	$3.4 \times 10^0$	2.49E+09	1.48	8602
	H-migrations or ring closure leads to high ring strain and are not competitive					



365

**Scheme 2.** Example reaction scheme for HOM formation after H-abstraction in limonene, based mostly on SAR prediction and starting at the fastest of 5 allylic H-abstraction sites. Direct autoxidation of the nascent RO<sub>2</sub> is slow,  $k \sim 10^{-2} \text{ s}^{-1}$ , and formation of an alkoxy radical is to be expected immediately or after very few autoxidation steps, especially in high NO conditions. Once the ring structure is broken, fast autoxidation steps are accessible. All RO<sub>2</sub> intermediates have competing reactions (not shown) under current conditions with HO<sub>2</sub> (forming hydroperoxides) and NO (forming alkoxy radicals and nitrates). Alkoxy radicals formed thus can fragment, or continue autoxidation after ring breaking or fast migration of an hydroperoxide H-atom, forming a wider variety of HOM.

370

### 3.3.3 Relative contribution of OH addition versus OH H-abstraction

As C<sub>10</sub>H<sub>15</sub>O<sub>x</sub> (x=7-12) is formed via the OH H-abstraction pathway and C<sub>10</sub>H<sub>17</sub>O<sub>x</sub> is formed via OH addition, we can compare the relative importance of these two pathways via the ratios of C<sub>10</sub>H<sub>15</sub>O<sub>x</sub> to C<sub>10</sub>H<sub>17</sub>O<sub>x</sub> radicals and their termination products. At low NO, the ratio of the concentrations of C<sub>10</sub>H<sub>15</sub>O<sub>x</sub> to C<sub>10</sub>H<sub>17</sub>O<sub>x</sub> was 0.47 and the ratios of the concentrations of C<sub>10</sub>H<sub>15</sub>O<sub>x</sub> related termination products carbonyls (C<sub>10</sub>H<sub>14</sub>O<sub>x</sub>) and organic nitrates (C<sub>10</sub>H<sub>15</sub>NO<sub>x</sub>) to C<sub>10</sub>H<sub>17</sub>O<sub>x</sub> related termination products carbonyls (C<sub>10</sub>H<sub>16</sub>O<sub>x</sub>) and organic nitrates (C<sub>10</sub>H<sub>17</sub>NO<sub>x</sub>) are 0.9 and 0.7, respectively (Fig. 3c). At high NO, the ratio of the concentrations of C<sub>10</sub>H<sub>15</sub>O<sub>x</sub> to C<sub>10</sub>H<sub>17</sub>O<sub>x</sub> was ~2 (Fig. 3) and the corresponding ratios of the concentrations of C<sub>10</sub>H<sub>15</sub>O<sub>x</sub> related termination products to C<sub>10</sub>H<sub>17</sub>O<sub>x</sub> related termination products are 0.6 and 0.5, respectively (Fig. 3c). Note that C<sub>10</sub>H<sub>16</sub>O<sub>x</sub> can be termination products from either C<sub>10</sub>H<sub>15</sub>O<sub>x</sub> or C<sub>10</sub>H<sub>17</sub>O<sub>x</sub> radicals depending on whether they contain hydroxyl/hydroperoxyl (ROH/ROOH) or carbonyl (RC=O) functionalities; the relative substituent contributions in C<sub>10</sub>H<sub>16</sub>O<sub>x</sub> were quantified using the method described in Sect. 2.2. The concentrations of C<sub>10</sub>H<sub>16</sub>O<sub>x</sub> and C<sub>10</sub>H<sub>18</sub>O<sub>x</sub> (alcohol and hydroperoxide products), formed from C<sub>10</sub>H<sub>15</sub>O<sub>x</sub> and C<sub>10</sub>H<sub>17</sub>O<sub>x</sub> radicals respectively, were found to be negligible, and we

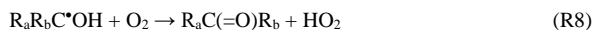
380



385 can assign  $C_{10}H_{16}O_x$  products as carbonyls formed from the OH addition  $C_{10}H_{17}O_x^\bullet$  radicals. Overall, the  $C_{10}H_{15}O_x^\bullet$  related products formed via the H-abstraction channel contribute 43% and 46% of  $C_{10}$  HOM monomer respectively at low and high NO.

The ratio between products of  $C_{10}H_{15}O_x^\bullet$  and  $C_{10}H_{17}O_x^\bullet$  radicals is stable at both low and high NO (Fig. 4), except for a small decrease at the early reaction times under low NO conditions (Fig. 4c), albeit with large error. At the same time, the nitrate ratio  $C_{10}H_{15}NO_x/C_{10}H_{17}NO_x$  is lower than that of  $C_{10}H_{14}O_x/C_{10}H_{16}O_x$ , which indicates that carbonyl production from  $C_{10}H_{15}O_x^\bullet$  is more efficient than from  $C_{10}H_{17}O_x^\bullet$ . The concentration of peroxy radicals  $C_{10}H_{15}O_x^\bullet$  and the related termination products  $C_{10}H_{14}O_x$  and  $C_{10}H_{15}NO_x$  were comparable to  $C_{10}H_{17}O_x^\bullet$  and its corresponding products, illustrating the significant role of the H-abstraction pathway in the HOM formation from limonene oxidation by OH at low and high NO. The high yield of carbonyl products in the absence of alcohol products indicates that here carbonyls are not formed from  $RO_2 + RO_2$  reactions (see also Figure S2), but rather from termination reactions in  $HOOQOO^\bullet$  radicals eliminating an OH radical after an  $\alpha$ -OOH H-atom migration, forming  $O=QOOH$ . This observation is in agreement with recent findings for  $\alpha$ -pinene (Shen et al., 2022) and previous studies (Miller et al., 2005; Taatjes, 2006; Rissanen et al., 2014; Bianchi et al., 2019).

The large contribution of  $C_{10}H_{15}O_x^\bullet$  related products to HOM formation can be attributed to the significant contribution of H-abstraction by OH in the initial step. While OH addition is believed to be the major initiation channel in the reaction of limonene+OH and H-abstraction is often ignored in current chemical mechanisms (e.g. MCM v3.3.1), H-abstraction by OH is clearly not negligible. Already previous studies have suggested that H-abstraction can be a significant reaction pathway with  $\sim 34 \pm 8\%$  branching ratio for the reactions of limonene with OH radical at 298 K (Rio et al., 2010; Dash and Rajakumar, 2015), and  $33.6 \pm 4.8\%$  at 293 K (Braure et al., 2014). We found that the ratio of  $C_{10}H_{15}O_x^\bullet$  to  $C_{10}H_{17}O_x^\bullet$  at high NO condition was higher than 2, emphasizing the importance of H-abstraction. A similar abundance of carbonyls ( $C_{10}H_{14}O_x$ ) and organic nitrates ( $C_{10}H_{15}NO_x$ ) stemming from  $C_{10}H_{15}O_x^\bullet$  radicals compared to their counterparts  $C_{10}H_{16}O_x$  and  $C_{10}H_{17}NO_x$  from  $C_{10}H_{17}O_x^\bullet$  at both low and high NO levels (Fig. 3) likewise indicates that H-abstraction in the first step of limonene oxidation by OH is important for the subsequent oxidation. Moreover, the high relative yields of HOM from the H-abstraction channel compared to its contribution in the limonene+OH initiation reaction can be tentatively attributed to the difference in the autoxidation mechanisms (Scheme 1 and 2). Many of the autoxidation channels following OH addition lead efficiently to termination products (Scheme 1) and requires additional OH reactions to undergo further oxidation, whereas the  $RO_2$  formed from H-abstraction readily lend themselves for a sequence of  $O_2$  additions, once the ring structure is broken. The key difference is the presence of  $\beta$ -OH and  $\beta$ -OOH moieties in the alkoxy in the OH addition branch, which can form  $\alpha$ -OH alkyl radicals and  $\alpha$ -OOH alkyl radicals in fragmentation steps and further lead to  $HO_2$  formation from  $\alpha$ -OH alkyl radicals +  $O_2$  (R8) or by regeneration of OH from  $\alpha$ -OOH alkyl radicals (R9), thus preventing ring breaking without termination of the autoxidation chain:



In contrast, the alkoxy step after H-abstraction breaks the 6-membered ring to a new  $RO_2$ , enhancing autoxidation (scheme 2). The propensity of the  $RO_2$  from OH adducts to terminate the autoxidation chain, especially at higher NO where  $\beta$ -OH and  $\beta$ -OOH alkoxy decomposition is prevalent, then allows the H-abstraction  $RO_2$  to play a more dominant role. Contrary to our earlier studies on  $\beta$ -pinene or limonene with  $NO_3$  (Shen et al., 2021; Guo et al., 2022), where we were able to assign  $RO_2$  and products to first-, second-, or later-generation chemistry, no such clear n-th generation distinction can be made for the HOM mass spectrum traces in the limonene+OH system. This suggests that the observed HOMs are a mixture formed in several generations of OH-initiation reactions, and lends further credence to our proposal that termination reactions requiring additional OH reactions are hampering the main OH addition channel from efficiently producing HOMs.

To our knowledge, no previous studies have observed  $C_{10}H_{15}O_x^\bullet$  radicals in limonene oxidation by OH, although in ozonolysis the formation of  $C_{10}H_{15}O_x^\bullet$  and their termination products including  $C_{10}H_{14-16}O_{6-10}$  monomers and  $C_{18-20}H_{28-34}O_{6-16}$



was observed (Hammes et al., 2019; Tomaz et al., 2021), and field observations have shown the presence of  $C_{10}H_{15}O_x$  radicals in the atmosphere (Yan et al., 2020; Massoli et al., 2018). Recent theoretical work from Piletic and Kleindienst (2022) concluded that H-abstraction does not contribute to HOM in limonene+OH, but this study did not account for any alkoxy-peroxy autoxidation steps. Our study, then, shows for the first time that H-abstraction significantly contributes to HOM formation in the reaction of limonene+OH under reaction conditions that allow formation of alkoxy radicals such as by reaction with NO,  $RO_2$  or  $NO_3$ , as commonly found in the atmosphere.

### 3.3.4 Comparison against $\alpha$ -pinene HOM formation

In our previous study, we have observed the large contribution of hydrogen abstraction OH to HOM formation in the oxidation of  $\alpha$ -pinene by OH (Shen et al., 2022). There, at low NO (0.03-0.1 ppb), the ratio of HOM formed from hydrogen abstraction relative to OH addition increased in the beginning of the experiment and had a delay of 3-5 min before reaching 1:1. At high NO (~20 ppb), an enhancement of the HOM yields formed through H-abstraction was observed, both absolute and relative to the HOM formed through OH addition. Alkoxy radical steps were found to be a prerequisite for the autoxidation and thus HOM formation in the hydrogen abstraction pathway. As discussed in Sect. 3.3.3, in limonene+OH oxidation, the ratios of  $C_{10}H_{14}O_x$  to  $C_{10}H_{16}O_x$  and of  $C_{10}H_{15}NO_x$  to  $C_{10}H_{17}NO_x$  and the time series of the ratios were similar at low and high NO. These results indicate that the rate of autoxidation for both the limonene H-abstraction and OH addition channels are affected to a similar extent by competing bimolecular reactions such as with NO. This contrasts with the enhancement of the HOM yield through H-abstraction in the  $\alpha$ -pinene system with increasing NO concentrations (Shen et al., 2022).

The different kinetic behaviour relative to competing reactions can be attributed to the different molecular structures of  $\alpha$ -pinene and limonene.  $\alpha$ -pinene is a bicyclic rigid molecule, and the  $RO_2$  formed from H-abstraction do not undergo autoxidation as rate coefficients are  $\leq 10^{-4} s^{-1}$  (Shen et al., 2022). Even after breaking the first ring in an alkoxy step, autoxidation rates remain fairly slow,  $\leq 10^{-1} s^{-1}$ , requiring a second alkoxy step with ring breaking before fast autoxidation occurs. This makes HOM formation through H-abstraction sensitive to the NO concentration in the first few steps. In contrast, limonene has only a single 6-ring and only a single alkoxy ring breaking is needed to allow fast autoxidation in the resulting non-cyclic molecule. Moreover, the primary  $RO_2$  from H-abstraction of limonene can still undergo some slow autoxidation, with rates  $\sim 10^{-2} s^{-1}$  (see Table 1), and possibly break the ring at a later stage (see Scheme 2). Overall, then, autoxidation in limonene system after H-abstraction is more competitive even at lower NO than  $\alpha$ -pinene system. We should note, though, that the low-NO experiments of limonene oxidation were performed at NO concentrations that were higher by a factor 2 to 7 compared to the low-NO experiment for  $\alpha$ -pinene (~0.2 ppb and 0.03-0.1 ppb, respectively); we speculate that an NO-dependence of the abstraction versus addition channel ratio might become apparent even in the limonene system at strongly reduced NO levels. The higher absolute contribution of HOM from the H-abstraction channel in limonene (H-abstraction related HOM yields: 1.3% low NO and 0.38% at high NO, shown in Sect. 3.4) is also affected by the higher branching ratio of H-abstraction in limonene+OH, ~34% (Rio et al., 2010; Dash and Rajakumar, 2015), compared to  $\alpha$ -pinene+OH, ~11% (Vereecken and Peeters, 2000).

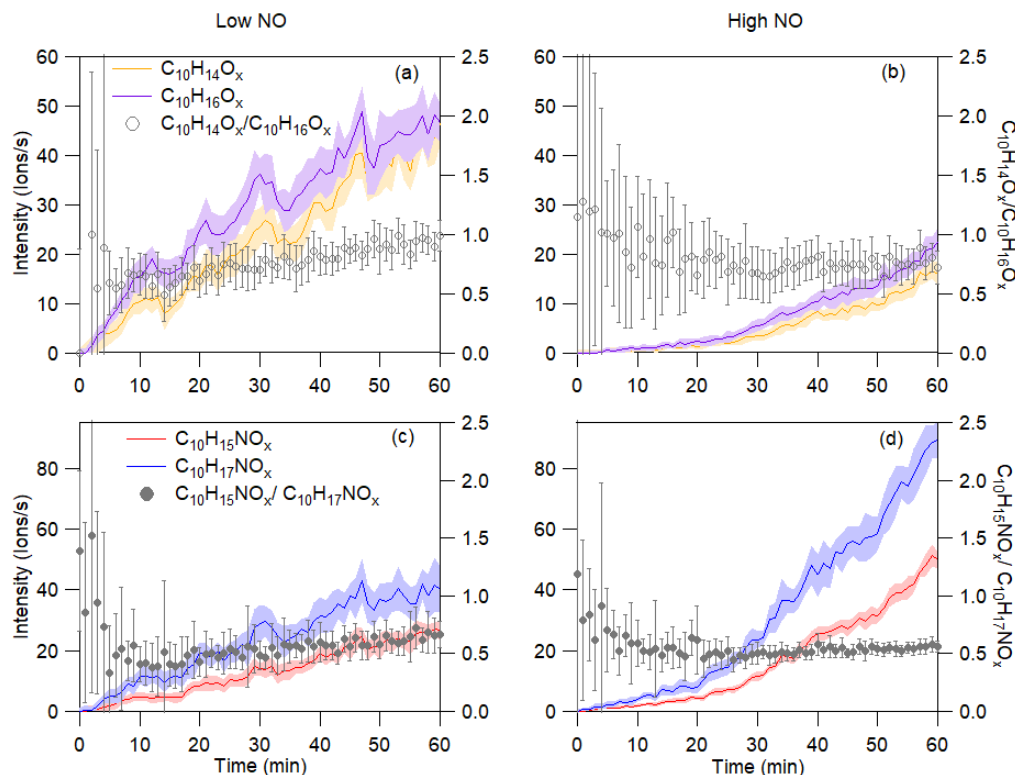


**Figure 4.** Time series of  $C_{10}H_{15}O_x$  and  $C_{10}H_{17}O_x$  related families of carbonyls and organic nitrates during the first 60 min of the experiments. The carbonyl families  $C_{10}H_{14}O_x$  (yellow),  $C_{10}H_{16}O_x$  (purple), and their concentration ratio ( $C_{10}H_{14}O_x / C_{10}H_{16}O_x$ ) are shown for (a) low and (b) high NO experiments. Time series for organic nitrate families  $C_{10}H_{15}NO_x$  (red) and  $C_{10}H_{17}NO_x$  (blue), and concentration ratio of  $C_{10}H_{15}NO_x / C_{10}H_{17}NO_x$ , are similarly demonstrated in (c) for low NO and (d) high NO experiments. All data are averaged to 1 min and the error bar represents one standard deviation.

### 3.4 HOM yield

470 The HOM yields during the first 60 min was estimated to be  $3.0^{+3.9}_{-1.6}\%$  and  $0.82^{+1.1}_{-0.44}\%$  at low and high NO respectively. In brief, the uncertainty (-54%/+128%) was estimated from the HOM signal intensity, VOC concentration, and calibration coefficient of  $H_2SO_4$  as discussed by Zhao et al (2021) (see Supplement S1). The lower HOM yields at high NO can be partly attributed to lower fractions of dimer products for the inhibitory effect of  $NO_x$  as discussed above (Sect. 3.2.3). Within the uncertainty, the HOM yield at high NO in this study is comparable to the HOM yield ( $0.93 \pm 0.47\%$ ) from the photooxidation of limonene in a previous study (Jokinen et al., 2015). The difference in yield at low NO from (Jokinen et al., 2015) may be attributed to different experimental methods and conditions. For example, Jokinen et al. (2015) derived HOM yield from OH oxidation indirectly by comparing the HOM yield in ozonolysis with and without OH scavenger while in this study we determined HOM yield directly for the oxidation of limonene by OH. In ozonolysis, the cross reactions of  $RO_2$  formed from ozonolysis and OH oxidation may produce accretion products thus possibly confounding the results. By directly measuring

475

480 HOM yield in the oxidation of limonene by OH, such influence is avoided. The NO concentration might be also different between our study and Jokinen et al. (2015). Additionally, the HOM yields related to H-abstraction were further determined to be  $1.3^{+1.7}_{-0.71}\%$  at low NO and  $0.38^{+0.48}_{-0.20}\%$  at high NO, when assuming that the ratio of all HOM from H-abstraction to those from OH addition is equal to the corresponding ratio for  $C_{10}$ -monomers.



#### 4 Conclusions and atmospheric implications

485 In this study, the HOM products in the oxidation of limonene with OH were investigated by using a  $\text{NO}_3^-$ -CIMS in the SAPHIR chamber in Jülich. A large number of HOM monomers ( $\text{C}_{6-10}$ ) and dimers ( $\text{C}_{17-20}$ ) were detected and classified according to the number of carbon atoms. Among HOM products, the proportion of HOM monomers is far higher than dimers in both low and high NO condition.  $\text{C}_{10}$  HOM were the most abundant monomers at both low and high NO. At low NO, the fraction of organic nitrates (33%) was lower than that of non-nitrate HOM (67%). At high NO, a higher fraction of 45% were observed  
490 for organic nitrates. Two major  $\text{RO}_2$  radical families,  $\text{C}_{10}\text{H}_{15}\text{O}_x^\bullet$  and  $\text{C}_{10}\text{H}_{17}\text{O}_x^\bullet$ , were identified. While  $\text{C}_{10}\text{H}_{17}\text{O}_x^\bullet$  were formed via OH addition to a double bond,  $\text{C}_{10}\text{H}_{15}\text{O}_x^\bullet$  is proposed to be formed via H-abstraction by OH on the basis of its molecular formula and the available literature. Although the concentrations of  $\text{C}_{10}\text{H}_{15}\text{O}_x^\bullet$  related products were less than  $\text{C}_{10}\text{H}_{17}\text{O}_x^\bullet$  related products, they remained at a comparable magnitude (38.6% vs 47.9% at low NO and 30.2% vs 61.5% at high NO). The formation pathways of  $\text{C}_{10}\text{H}_{15}\text{O}_x^\bullet$  and  $\text{C}_{10}\text{H}_{17}\text{O}_x^\bullet$  were proposed on the basis of observed signal intensity, theoretical kinetic  
495 calculations, and structure activity relationships (SARs) for autoxidation. At both low and high NO, H-abstraction by OH contributes a significant fraction of HOM (43% and 46% of  $\text{C}_{10}$  HOM monomer, respectively), demonstrating that H-abstraction is important to the formation of HOM in the oxidation of limonene with OH radical, and contributes more than expected given the ~34% contribution in the initiation reaction. The key mechanistic difference between OH addition and H-abstraction pathways is that the former does not readily lead to breaking of the six-membered ring without chain termination,  
500 whereas H-abstraction leads to fast first-generation autoxidation after an alkoxy-peroxy ring breaking step.  $\text{C}_6$ - $\text{C}_9$  monomers are proposed to be formed via fragmentation of alkoxy radicals and  $\text{C}_{17}$ - $\text{C}_{20}$  dimers are proposed to be formed via accretion reactions.

The yields of total HOM are estimated to be  $3.04^{+3.89}_{-1.64}\%$  and  $0.82^{+1.05}_{-0.44}\%$  in low and high NO condition. Although the HOM yields in the oxidation of limonene with OH in this study are lower than that in the ozonolysis of limonene (Jokinen et al.,  
505 2015), the corresponding SOA yields assuming irreversible condensation of HOM can be as high as 6.6% and 1.6% at low NO and high NO, respectively. Similarly, while the gas-phase dimers observed in this study are clearly lower than monomers in abundance, dimers may also be very efficient at condensing onto newly formed particles due to their large size and low volatility. These HOM dimer products are known to have an extremely low volatility due to their size and high degree of oxidation (Tröstl et al., 2016).

510 This study highlights the importance of the pathway of H-abstraction by OH in competition to OH addition to double bonds in the same molecule at least for HOM formation, which has largely been neglected in current chemical mechanisms. The importance of H-abstraction pathway to HOM formation also in  $\alpha$ -pinene+OH oxidation has been shown in our recent study (Shen et al., 2022), and recent experimental work by Williams et al. (2022). H-abstraction in the case of limonene+OH is more prominent than for  $\alpha$ -pinene+OH, but the OH abstraction pathway is important in both systems suggesting its importance in  
515 other terpenes or even other unsaturated species. We propose that in order to accurately simulate HOM formation from oxidation of limonene by OH, H-abstraction should be considered in chemical mechanisms of atmospheric models. Considering the key role HOM in SOA particle formation and growth, this study further enables more accurate simulation of chemical composition and concentrations of secondary organic aerosol as well as growth of particles to CCN size in order to assess the impact of SOA on climate.

520 The experiments in this study were conducted at ambient relevant conditions by using limonene and OH concentrations at ambient levels and using natural sunlight. The major  $\text{RO}_2$  loss rate in all experiments is via  $\text{RO}_2+\text{NO}$  with a significant contribution of  $\text{RO}_2+\text{HO}_2$  after ~2 h at low NO. Therefore, the HOM composition and formation pathway can represent a large part of the daytime continental environment. The low NO conditions are representative of forested regions with biogenic monoterpene emissions and influenced by anthropogenic emissions and of rural regions. The experiments at high NO in this  
525 study are relevant for the reactions of limonene with OH in urban environment as limonene is also a major component of VCP besides biogenic sources (Nazaroff and Weschler, 2004; Rossignol et al., 2013; Waring, 2016; Gkatzelis et al., 2021).



The fraction of organic nitrate HOM, such as C<sub>10</sub>H<sub>15</sub>NO<sub>x</sub> and C<sub>10</sub>H<sub>17</sub>NO<sub>x</sub>, was significant in the total HOM products in both low and high NO conditions examined, highlighting the importance of organic nitrates (ONs). Even at ~0.2 ppb NO, ONs account for a large part (29%) of HOM. ONs are important in the atmosphere as they can serve as an NO<sub>x</sub> reservoir (Ng et al., 2017). Highly functionalized ONs have been inferred to be capable of strongly partitioning to the particle phase (Perraud et al., 2012; Ng et al., 2007). The significant amounts of monoterpene-derived ONs that were observed in field campaigns (Massoli et al., 2018; Huang et al., 2019; Lee et al., 2016) indicate that ONs make up a significant fraction of SOA. The abundant presence of ONs highlights the importance of NO<sub>x</sub>-driven chemistry in daytime. In most of the continental environment influenced by monoterpene, ONs then likely contribute a large fraction of HOM and SOA, and contribute the organic nitrates and particle formation in the atmosphere.

### Acknowledgement

H. Luo, H. Shen, and D. Zhao would like to thank the funding support of National Natural Science Foundation of China (No. 41875145), Science and Technology Commission of Shanghai Municipality (No. 20230711400), and Shanghai International Science and Technology Partnership Project (No. 21230780200). Sungah Kang, Astrid Kiendler-Scharr, and Thomas F. Mentel acknowledge the support by the EU Project FORCeS (grant agreement no. 821205).

### Data availability

The supplement provides additional figures and tables, and further information on the CIMS calibration and HOM monomers and dimers with reduced carbon number.

The quantum chemical data (geometries, vibrational wavenumbers, rotational constants, energies, and partition functions) can be found under <https://doi.org/10.26165/JUELICH-DATA/9JVHEK>. [Reviewers: the quantum chemical data can be accessed for reviewing purposes under URL <https://data.fz-juelich.de/privateurl.xhtml?token=60754bd4-d921-449c-9210-7b24839a67ce>]

### References

- Alecu, I. M., Zheng, J., Zhao, Y., and Truhlar, D. G.: Computational thermochemistry\_ scale factor databases and scale factors for vibrational frequencies obtained from electronic model chemistries, *J Chem Theory Comput*, 6, 2872-2887, 2010.
- Bartlett, R. J. and Purvis, G. D.: Many-Body Perturbation-Theory, Coupled-Pair Many-Electron Theory, and Importance of Quadruple Excitations for Correlation Problem, *International Journal of Quantum Chemistry*, 14, 561-581, DOI 10.1002/qua.560140504, 1978.
- Berndt, T.: Peroxy Radical Processes and Product Formation in the OH Radical-Initiated Oxidation of alpha-Pinene for Near-Atmospheric Conditions, *J Phys Chem A*, 125, 9151-9160, 10.1021/acs.jpca.1c05576, 2021.
- Berndt, T., Mentler, B., Scholz, W., Fischer, L., Herrmann, H., Kulmala, M., and Hansel, A.: Accretion Product Formation from Ozonolysis and OH Radical Reaction of alpha-Pinene: Mechanistic Insight and the Influence of Isoprene and Ethylene, *Environ Sci Technol*, 52, 11069-11077, 10.1021/acs.est.8b02210, 2018.
- Berndt, T., Richters, S., Jokinen, T., Hyttinen, N., Kurtén, T., Otkjær, R. V., Kjaergaard, H. G., Stratmann, F., Herrmann, H., Sipilä, M., Kulmala, M., and Ehn, M.: Hydroxyl radical-induced formation of highly oxidized organic compounds, *Nat Commun*, 7, 13677, 10.1038/ncomms13677, 2016.
- Bianchi, F., Kurtén, T., Riva, M., Mohr, C., Rissanen, M. P., Roldin, P., Berndt, T., Crouse, J. D., Wennberg, P. O., Mentel, T. F., Wildt, J., Junninen, H., Jokinen, T., Kulmala, M., Worsnop, D. R., Thornton, J. A., Donahue, N., Kjaergaard, H. G., and Ehn, M.: Highly Oxygenated Organic Molecules (HOM) from Gas-Phase Autoxidation Involving Peroxy Radicals: A Key Contributor to Atmospheric Aerosol, *Chem Rev*, 119, 3472-3509, 10.1021/acs.chemrev.8b00395, 2019.
- Braure, T., Bedjanian, Y., Romanias, M. N., Morin, J., Riffault, V., Tomas, A., and Coddeville, P.: Experimental study of the reactions of limonene with OH and OD radicals: kinetics and products, *J Phys Chem A*, 118, 9482-9490, 10.1021/jp507180g, 2014.
- Chen, X. and Hopke, P. K.: A chamber study of secondary organic aerosol formation by limonene ozonolysis, *Indoor Air*, 20, 320-328, 10.1111/j.1600-0668.2010.00656.x, 2010.
- Crouse, J. D., Nielsen, L. B., Jørgensen, S., Kjaergaard, H. G., and Wennberg, P. O.: Autoxidation of Organic Compounds in the Atmosphere, *J Phys Chem Lett*, 4, 3513-3520, 10.1021/jz4019207, 2013.



- Dash, M. R. and Rajakumar, B.: Theoretical investigations of the gas phase reaction of limonene (C<sub>10</sub>H<sub>16</sub>) with OH radical, *Mol Phys*, 113, 3202-3215, 10.1080/00268976.2015.1014002, 2015.
- Dunning, T. H.: Gaussian basis sets for use in correlated molecular calculations. I. The atoms boron through neon and hydrogen, *J Chem Phys*, 90, 1007-1023, 10.1063/1.456153, 1989.
- Dunning, T. H., Peterson, K. A., and Wilson, A. K.: Gaussian basis sets for use in correlated molecular calculations. X. The atoms aluminum through argon revisited, *J Chem Phys*, 114, 9244-9253, 10.1063/1.1367373, 2001.
- 580 Eckart, C.: The Penetration of a Potential Barrier by Electrons, *Phys Rev*, 35, 1303-1309, 10.1103/PhysRev.35.1303, 1930.
- Eddingsaas, N. C., Loza, C. L., Yee, L. D., Seinfeld, J. H., and Wennberg, P. O.:  $\alpha$ -pinene photooxidation under controlled chemical conditions – Part I: Gas-phase composition in low- and high-NO<sub>x</sub> environments, *Atmos Chem Phys*, 12, 6489-6504, 10.5194/acp-12-6489-2012, 2012.
- 585 Ehn, M., Berndt, T., Wildt, J., and Mentel, T.: Highly Oxygenated Molecules from Atmospheric Autoxidation of Hydrocarbons: A Prominent Challenge for Chemical Kinetics Studies, *Int J Chem Kinet*, 49, 821-831, 10.1002/kin.21130, 2017.
- Ehn, M., Kleist, E., Junninen, H., Petäjä, T., Lönn, G., Schobesberger, S., Dal Maso, M., Trimborn, A., Kulmala, M., Worsnop, D. R., Wahner, A., Wildt, J., and Mentel, T. F.: Gas phase formation of extremely oxidized pinene reaction products in chamber and ambient air, *Atmos Chem Phys*, 12, 5113-5127, 10.5194/acp-12-5113-2012, 2012.
- 590 Ehn, M., Thornton, J. A., Kleist, E., Sipilä, M., Junninen, H., Pullinen, I., Springer, M., Rubach, F., Tillmann, R., Lee, B., Lopez-Hilfiker, F., Andres, S., Acir, I. H., Rissanen, M., Jokinen, T., Schobesberger, S., Kangasluoma, J., Kontkanen, J., Nieminen, T., Kurtén, T., Nielsen, L. B., Jørgensen, S., Kjaergaard, H. G., Canagaratna, M., Maso, M. D., Berndt, T., Petäjä, T., Wahner, A., Kerminen, V. M., Kulmala, M., Worsnop, D. R., Wildt, J., and Mentel, T. F.: A large source of low-volatility secondary organic aerosol, *Nature*, 506, 476-479, 10.1038/nature13032, 2014.
- 595 Finlayson-Pitts, B. J. and Pitts, J. N. J.: *Chemistry of the Upper and Lower Atmosphere: Theory, Experiments, and Applications*, Academic Press, San Diego, San Francisco, New York, Boston London, Sydney Tokyo2000.
- Friedman, B. and Farmer, D. K.: SOA and gas phase organic acid yields from the sequential photooxidation of seven monoterpenes, *Atmos Environ*, 187, 335-345, 10.1016/j.atmosenv.2018.06.003, 2018.
- 600 Frisch, M. J., Trucks, G. W., Schlegel, H. B., and G. E. Scuseria, M. A. R., J. R. Cheeseman, G. Scalmani, V. Barone, G. A. Petersson, H. Nakatsuji, X. Li, M. Caricato, A. V. Marenich, J. Bloino, B. G. Janesko, R. Gomperts, B. Mennucci, H. P. Hratchian, J. V. Ortiz, A. F. Izmaylov, J. L. Sonnenberg, Williams, F. Ding, F. Lipparini, F. Egidi, J. Goings, B. Peng, A. Petrone, T. Henderson, D. Ranasinghe, V. G. Zakrzewski, J. Gao, N. Rega, G. Zheng, W. Liang, M. Hada, M. Ehara, K. Toyota, R. Fukuda, J. Hasegawa, M. Ishida, T. Nakajima, Y. Honda, O. Kitao, H. Nakai, T. Vreven, K. Throssell, J. A. Montgomery Jr., J. E. Peralta, F. Ogliaro, M. J. Bearpark, J. J. Heyd, E. N. Brothers, K. N. Kudin, V. N. Staroverov, T. A. Keith, R. Kobayashi, J. Normand, K. Raghavachari, A. P. Rendell, J. C. Burant, S. S. Iyengar, J. Tomasi, M. Cossi, J. M. Millam, M. Klene, C. Adamo, R. Cammi, J. W. Ochterski, R. L. Martin, K. Morokuma, O. Farkas, J. B. Foresman, D. J. Fox.: *Gaussian 09 Revision E.01*, Gaussian Inc., [code], 2016.
- 605 Fuchs, H., Dorn, H.-P., Bachner, M., Bohn, B., Brauers, T., Gomm, S., Hofzumahaus, A., Holland, F., Nehr, S., Rohrer, F., Tillmann, R., and Wahner, A.: Comparison of OH concentration measurements by DOAS and LIF during SAPHIR chamber experiments at high OH reactivity and low NO concentration, *Atmos Meas Tech*, 5, 1611-1626, 10.5194/amt-5-1611-2012, 2012.
- 610 Gkatzelis, G. I., Coggon, M. M., McDonald, B. C., Peischl, J., Gilman, J. B., Aikin, K. C., Robinson, M. A., Canonaco, F., Prevot, A. S. H., Trainer, M., and Warneke, C.: Observations Confirm that Volatile Chemical Products Are a Major Source of Petrochemical Emissions in U.S. Cities, *Environ Sci Technol*, 55, 4332-4343, 10.1021/acs.est.0c05471, 2021.
- Goerigk, L., Hansen, A., Bauer, C., Ehrlich, S., Najibi, A., and Grimme, S.: A look at the density functional theory zoo with the advanced GMTKN55 database for general main group thermochemistry, kinetics and noncovalent interactions, *Phys Chem Chem Phys*, 19, 32184-32215, 10.1039/c7cp04913g, 2017.
- 615 Gong, Y., Chen, Z., and Li, H.: The oxidation regime and SOA composition in limonene ozonolysis: roles of different double bonds, radicals, and water, *Atmos Chem Phys*, 18, 15105-15123, 10.5194/acp-18-15105-2018, 2018.
- Griffin, R. J., Cocker, D. R., Flagan, R. C., and Seinfeld, J. H.: Organic aerosol formation from the oxidation of biogenic hydrocarbons, *J Geophys Res*, 104, 3555-3567, 10.1029/1998jd100049, 1999.
- 620 Grimme, S., Ehrlich, S., and Goerigk, L.: Effect of the damping function in dispersion corrected density functional theory, *J Comput Chem*, 32, 1456-1465, 10.1002/jcc.21759, 2011.
- Guenther, A. B., Jiang, X., Heald, C. L., Sakulyanontvittaya, T., Duhl, T., Emmons, L. K., and Wang, X.: The Model of Emissions of Gases and Aerosols from Nature version 2.1 (MEGAN2.1): an extended and updated framework for modeling biogenic emissions, *Geosci Model Dev*, 5, 1471-1492, 10.5194/gmd-5-1471-2012, 2012.
- 625 Guo, Y., Shen, H., Pullinen, I., Luo, H., Kang, S., Vereecken, L., Fuchs, H., Hallquist, M., Acir, I.-H., Tillmann, R., Rohrer, F., Wildt, J., Kiendler-Scharr, A., Wahner, A., Zhao, D., and Mentel, T. F.: Identification of highly oxygenated organic molecules and their role in aerosol formation in the reaction of limonene with nitrate radical, *Atmos Chem Phys*, 22, 11323-11346, 10.5194/acp-2022-85, 2022.
- 630 Hakola, H., Arey, J., Aschmann, S. M., and Atkinson, R.: Product Formation from the Gas-Phase Reactions of Oh Radicals and O<sub>3</sub> with a Series of Monoterpenes, *J Atmos Chem*, 18, 75-102, Doi 10.1007/Bf00694375, 1994.
- Hallquist, M., Wenger, J. C., Baltensperger, U., Rudich, Y., Simpson, D., Claeys, M., Dommen, J., Donahue, N. M., George, C., Goldstein, A. H., Hamilton, J. F., Herrmann, H., Hoffmann, T., Iinuma, Y., Jang, M., Jenkin, M. E., Jimenez, J. L., Kiendler-Scharr, A., Maenhaut, W., McFiggans, G., Mentel, T. F., Monod, A., Prévôt, A. S. H., Seinfeld, J. H., Surratt, J. D., Szmigielski, R., and Wildt, J.: The formation, properties and impact of secondary organic aerosol: current and emerging issues, *Atmos Chem Phys*, 9, 5155-5236, 2009.



- Hammes, J., Lutz, A., Mentel, T., Faxon, C., and Hallquist, M.: Carboxylic acids from limonene oxidation by ozone and hydroxyl radicals: insights into mechanisms derived using a FIGAERO-CIMS, *Atmos Chem Phys*, 19, 13037-13052, 10.5194/acp-19-13037-2019, 2019.
- 640 Huang, W., Saathoff, H., Shen, X., Ramisetty, R., Leisner, T., and Mohr, C.: Chemical Characterization of Highly Functionalized Organonitrates Contributing to Night-Time Organic Aerosol Mass Loadings and Particle Growth, *Environ Sci Technol*, 53, 1165-1174, 10.1021/acs.est.8b05826, 2019.
- Jaoui, M., Corse, E., Kleindienst, T. E., Offenberg, J. H., Lewandowski, M., and Edney, E. O.: Analysis of Secondary Organic Aerosol Compounds from the Photooxidation of d-Limonene in the Presence of NO<sub>x</sub> and their Detection in Ambient PM 2.5, *Environ Sci Technol*, 40, 3819-3828, 2006.
- 645 Jenkin, M. E., Saunders, S. M., and Pilling, M. J.: The tropospheric degradation of volatile organic compounds: a protocol for mechanism development, *Atmos Environ*, 31, 81-104, 1997.
- Jenkin, M. E., Valorso, R., Aumont, B., and Rickard, A. R.: Estimation of rate coefficients and branching ratios for reactions of organic peroxy radicals for use in automated mechanism construction, *Atmos Chem Phys*, 19, 7691-7717, 10.5194/acp-19-7691-2019, 2019.
- 650 Jenkin, M. E., Valorso, R., Aumont, B., Rickard, A. R., and Wallington, T. J.: Estimation of rate coefficients and branching ratios for gas-phase reactions of OH with aliphatic organic compounds for use in automated mechanism construction, *Atmos Chem Phys*, 18, 9297-9328, 10.5194/acp-18-9297-2018, 2018.
- Johnston, H. S. and Hecklen, J.: Tunnelling Corrections for Unsymmetrical Eckart Potential Energy Barriers, *J Phys Chem*, 66, 532-533, 1962.
- 655 Jokinen, T., Sipilä, M., Richters, S., Kerminen, V. M., Paasonen, P., Stratmann, F., Worsnop, D., Kulmala, M., Ehn, M., Herrmann, H., and Berndt, T.: Rapid autoxidation forms highly oxidized RO<sub>2</sub> radicals in the atmosphere, *Angew Chem Int Ed*, 53, 14596-14600, 10.1002/anie.201408566, 2014.
- Jokinen, T., Berndt, T., Makkonen, R., Kerminen, V. M., Junninen, H., Paasonen, P., Stratmann, F., Herrmann, H., Guenther, A. B., Worsnop, D. R., Kulmala, M., Ehn, M., and Sipilä, M.: Production of extremely low volatile organic compounds from biogenic emissions: Measured yields and atmospheric implications, *Proc Natl Acad Sci U S A*, 112, 7123-7128, 10.1073/pnas.1423977112, 2015.
- Jørgensen, S., Knap, H. C., Otkjær, R. V., Jensen, A. M., Kjeldsen, M. L., Wennberg, P. O., and Kjaergaard, H. G.: Rapid Hydrogen Shift Scrambling in Hydroperoxy-Substituted Organic Peroxy Radicals, *J Phys Chem A*, 120, 266-275, 10.1021/acs.jpca.5b06768, 2016.
- 665 Kanakidou, M., Seinfeld, J. H., Pandis, S. N., Barnes, I., Dentener, F. J., Facchini, M. C., Van Dingenen, R., Ervens, B., Nenes, A., Nielsen, C. J., Swietlicki, E., Putaud, J. P., Balkanski, Y., Fuzzi, S., Horth, J., Moortgat, G. K., Winterhalter, R., Myhre, C. E. L., Tsigaridis, K., Vignati, E., Stephanou, E. G., and Wilson, J.: Kanakidou\_Organic aerosol and global climate modelling: A review, *Atmos Chem Phys*, 5, 1053-1123, 2005.
- 670 Kenseth, C. M., Huang, Y., Zhao, R., Dalleska, N. F., Hethcox, J. C., Stoltz, B. M., and Seinfeld, J. H.: Synergistic O<sub>3</sub> + OH oxidation pathway to extremely low-volatility dimers revealed in beta-pinene secondary organic aerosol, *Proc Natl Acad Sci U S A*, 115, 8301-8306, 10.1073/pnas.1804671115, 2018.
- Kirkby, J., Duplissy, J., Sengupta, K., Frege, C., Gordon, H., Williamson, C., Heinritzi, M., Simon, M., Yan, C., Almeida, J., Tröstl, J., Nieminen, T., Ortega, I. K., Wagner, R., Adamov, A., Amorim, A., Bernhammer, A. K., Bianchi, F., Breitenlechner, M., Brilke, S., Chen, X., Craven, J., Dias, A., Ehrhart, S., Flagan, R. C., Franchin, A., Fuchs, C., Guida, R., Hakala, J., Hoyle, C. R., Jokinen, T., Junninen, H., Kangasluoma, J., Kim, J., Krapf, M., Kürten, A., Laaksonen, A., Lehtipalo, K., Makhmutov, V., Mathot, S., Molteni, U., Onnela, A., Peräkylä, O., Piel, F., Petäjä, T., Praplan, A. P., Pringle, K., Rap, A., Richards, N. A., Riipinen, I., Rissanen, M. P., Rondo, L., Sarnela, N., Schobesberger, S., Scott, C. E., Seinfeld, J. H., Sipilä, M., Steiner, G., Stozhkov, Y., Stratmann, F., Tomé, A., Virtanen, A., Vogel, A. L., Wagner, A. C., Wagner, P. E., Weingartner, E., Wimmer, D., Winkler, P. M., Ye, P., Zhang, X., Hansel, A., Dommen, J., Donahue, N. M., Worsnop, D. R., Baltensperger, U., Kulmala, M., Carslaw, K. S., and Curtius, J.: Ion-induced nucleation of pure biogenic particles, *Nature*, 533, 521-526, 10.1038/nature17953, 2016.
- 680 Knap, H. C. and Jørgensen, S.: Rapid Hydrogen Shift Reactions in Acyl Peroxy Radicals, *J Phys Chem A*, 121, 1470-1479, 10.1021/acs.jpca.6b12787, 2017.
- 685 Koch, S., Winterhalter, R., Uherek, E., Kolloff, A., Neeb, P., and Moortgat, G. K.: Formation of new particles in the gas-phase ozonolysis of monoterpenes, *Atmos Environ*, 34, 4031-4042, 2000.
- Krechmer, J. E., Coggon, M. M., Massoli, P., Nguyen, T. B., Crouse, J. D., Hu, W., Day, D. A., Tyndall, G. S., Henze, D. K., Rivera-Rios, J. C., Nowak, J. B., Kimmel, J. R., Mauldin, R. L., III, Stark, H., Jayne, J. T., Sipilä, M., Junninen, H., Clair, J. M. S., Zhang, X., Feiner, P. A., Zhang, L., Miller, D. O., Brune, W. H., Keutsch, F. N., Wennberg, P. O., Seinfeld, J. H., Worsnop, D. R., Jimenez, J. L., and Canagaratna, M. R.: Formation of Low Volatility Organic Compounds and Secondary Organic Aerosol from Isoprene Hydroxyhydroperoxide Low-NO Oxidation, *Environ Sci Technol*, 49, 10330-10339, 10.1021/acs.est.5b02031, 2015.
- 690 Lee, A., Goldstein, A. H., Kroll, J. H., Ng, N. L., Varutbangkul, V., Flagan, R. C., and Seinfeld, J. H.: Gas-phase products and secondary aerosol yields from the photooxidation of 16 different terpenes, *J Geophys Res*, 111, 10.1029/2006jd007050, 2006a.
- 695 Lee, A., Goldstein, A. H., Keywood, M. D., Gao, S., Varutbangkul, V., Bahreini, R., Ng, N. L., Flagan, R. C., and Seinfeld, J. H.: Gas-phase products and secondary aerosol yields from the ozonolysis of ten different terpenes, *J Geophys Res*, 111, 10.1029/2005jd006437, 2006b.
- Lee, B. H., Mohr, C., Lopez-Hilfiker, F. D., Lutz, A., Hallquist, M., Lee, L., Romer, P., Cohen, R. C., Iyer, S., Kurtén, T., Hu, W., Day, D. A., Campuzano-Jost, P., Jimenez, J. L., Xu, L., Ng, N. L., Guo, H., Weber, R. J., Wild, R. J., Brown, S. S.,
- 700



- Koss, A., de Gouw, J., Olson, K., Goldstein, A. H., Seco, R., Kim, S., McAvey, K., Shepson, P. B., Starn, T., Baumann, K., Edgerton, E. S., Liu, J., Shilling, J. E., Miller, D. O., Brune, W., Schobesberger, S., D'Ambro, E. L., and Thornton, J. A.: Highly functionalized organic nitrates in the southeast United States: Contribution to secondary organic aerosol and reactive nitrogen budgets, *Proc Natl Acad Sci U S A*, 113, 1516-1521, 10.1073/pnas.1508108113, 2016.
- 705 Massoli, P., Stark, H., Canagaratna, M. R., Krechmer, J. E., Xu, L., Ng, N. L., Mauldin, III., Roy L., Yan, C., Kimmel, J., Miszta, P. K., Jimenez, J. L., Jayne, J. T., and Worsnop, D. R.: Ambient Measurements of Highly Oxidized Gas-Phase Molecules during the Southern Oxidant and Aerosol Study (SOAS) 2013, *ACS Earth Space Chem*, 2, 653-672, 10.1021/acsearthspacechem.8b00028, 2018.
- McFiggans, G., Mentel, T. F., Wildt, J., Pullinen, I., Kang, S., Kleist, E., Schmitt, S., Springer, M., Tillmann, R., Wu, C., Zhao, D., Hallquist, M., Faxon, C., Le Breton, M., Hallquist, Å. M., Simpson, D., Bergström, R., Jenkin, M. E., Ehn, M., Thornton, J. A., Alfarra, M. R., Bannan, T. J., Percival, C. J., Priestley, M., Topping, D., and Kiendler-Scharr, A.: Secondary organic aerosol reduced by mixture of atmospheric vapours, *Nature*, 565, 587-593, 10.1038/s41586-018-0871-y, 2019.
- 710 Mentel, T. F., Springer, M., Ehn, M., Kleist, E., Pullinen, I., Kurtén, T., Rissanen, M., Wahner, A., and Wildt, J.: Formation of highly oxidized multifunctional compounds: autoxidation of peroxy radicals formed in the ozonolysis of alkenes – deduced from structure–product relationships, *Atmos Chem Phys*, 15, 6745-6765, 10.5194/acp-15-6745-2015, 2015.
- 715 Miller, J. A., Pilling, M. J., and Troe, J.: Unravelling combustion mechanisms through a quantitative understanding of elementary reactions, *P Combust Inst*, 30, 43-88, 10.1016/j.proci.2004.08.281, 2005.
- Møller, K. H., Bates, K. H., and Kjaergaard, H. G.: The Importance of Peroxy Radical Hydrogen-Shift Reactions in Atmospheric Isoprene Oxidation, *J Phys Chem A*, 123, 920-932, 10.1021/acs.jpca.8b10432, 2019.
- 720 Molteni, U., Simon, M., Heinritzi, M., Hoyle, C. R., Bernhammer, A.-K., Bianchi, F., Breitenlechner, M., Brilke, S., Dias, A., Duplissy, J., Frege, C., Gordon, H., Heyn, C., Jokinen, T., Kürten, A., Lehtipalo, K., Makhmutov, V., Petäjä, T., Pieber, S. M., Praplan, A. P., Schobesberger, S., Steiner, G., Stozhkov, Y., Tomé, A., Tröstl, J., Wagner, A. C., Wagner, R., Williamson, C., Yan, C., Baltensperger, U., Curtius, J., Donahue, N. M., Hansel, A., Kirkby, J., Kulmala, M., Worsnop, D. R., and Dommen, J.: Formation of Highly Oxygenated Organic Molecules from  $\alpha$ -Pinene Ozonolysis: Chemical Characteristics, Mechanism, and Kinetic Model Development, *ACS Earth Space Chem*, 3, 873-883, 10.1021/acsearthspacechem.9b00035, 2019.
- Nazaroff, W. W. and Weschler, C. J.: Cleaning products and air fresheners: exposure to primary and secondary air pollutants, *Atmos Environ*, 38, 2841-2865, 10.1016/j.atmosenv.2004.02.040, 2004.
- 730 Ng, N. L., Chhabra, P. S., Chan, A. W. H., Surratt, J. D., Kroll, J. H., Kwan, A. J., McCabe, D. C., Wennberg, P. O., Sorooshian, A., Murphy, S. M., Dalleska, N. F., Flagan, R. C., and Seinfeld, J. H.: Effect of NO<sub>x</sub> level on secondary organic aerosol (SOA) formation from the photooxidation of terpenes, *Atmos Chem Phys*, 7, 5159-5174, 2007.
- Ng, N. L., Brown, S. S., Archibald, A. T., Atlas, E., Cohen, R. C., Crowley, J. N., Day, D. A., Donahue, N. M., Fry, J. L., Fuchs, H., Griffin, R. J., Guzman, M. I., Herrmann, H., Hodzic, A., Iinuma, Y., Jimenez, J. L., Kiendler-Scharr, A., Lee, B. H., Luecken, D. J., Mao, J., McLaren, R., Mutzel, A., Osthoff, H. D., Ouyang, B., Picquet-Varrault, B., Platt, U., Pye, H. O. T., Rudich, Y., Schwantes, R. H., Shiraiwa, M., Stutz, J., Thornton, J. A., Tilgner, A., Williams, B. J., and Zaveri, R. A.: Nitrate radicals and biogenic volatile organic compounds: oxidation, mechanisms, and organic aerosol, *Atmos Chem Phys*, 17, 2103-2162, 10.5194/acp-17-2103-2017, 2017.
- 735 Novelli, A., Cho, C., Fuchs, H., Hofzumahaus, A., Rohrer, F., Tillmann, R., Kiendler-Scharr, A., Wahner, A., and Vereecken, L.: Experimental and theoretical study on the impact of a nitrate group on the chemistry of alkoxy radicals, *Phys Chem Chem Phys*, 23, 5474-5495, 10.1039/d0cp05555g, 2021.
- Nozière, B. and Vereecken, L.: Direct Observation of Aliphatic Peroxy Radical Autoxidation and Water Effects: An Experimental and Theoretical Study, *Angew Chem Int Ed*, 58, 13976-13982, 10.1002/anie.201907981, 2019.
- Pang, J. Y. S., Novelli, A., Kaminski, M., Acir, I.-H., Bohn, B., Carlsson, P. T. M., Cho, C., Dorn, H.-P., Hofzumahaus, A., Li, X., Lutz, A., Nehr, S., Reimer, D., Rohrer, F., Tillmann, R., Wegener, R., Kiendler-Scharr, A., Wahner, A., and Fuchs, H.: Investigation of the limonene photooxidation by OH at different NO concentrations in the atmospheric simulation chamber SAPHIR, *Atmos Chem Phys Discuss*, 10.5194/acp-2022-239, 2022.
- 745 Peeters, J., Vandenberk, S., Piessens, E., and Pultau, V.: H-atom abstraction in reactions of cyclic polyalkenes with OH, *Chemosphere*, 38, 1189-1195, 1999.
- Perraud, V., Bruns, E. A., Ezell, M. J., Johnson, S. N., Yu, Y., Alexander, M. L., Zelenyuk, A., Imre, D., Chang, W. L., Dabdub, D., Pankow, J. F., and Finlayson-Pitts, B. J.: Nonequilibrium atmospheric secondary organic aerosol formation and growth, *Proc Natl Acad Sci U S A*, 109, 2836-2841, 10.1073/pnas.1119909109, 2012.
- Piletic, I. R. and Kleindienst, T. E.: Rates and Yields of Unimolecular Reactions Producing Highly Oxidized Peroxy Radicals in the OH-Induced Autoxidation of  $\alpha$ -Pinene,  $\beta$ -Pinene, and Limonene, *J Phys Chem A*, 126, 88-100, 10.1021/acs.jpca.1c07961, 2022.
- 755 Praske, E., Otkjær, R. V., Crounse, J. D., Hethcox, J. C., Stoltz, B. M., Kjaergaard, H. G., and Wennberg, P. O.: Intramolecular Hydrogen Shift Chemistry of Hydroperoxy-Substituted Peroxy Radicals, *J Phys Chem A*, 123, 590-600, 10.1021/acs.jpca.8b09745, 2019.
- Pullinen, I., Schmitt, S., Kang, S., Sarrafzadeh, M., Schlag, P., Andres, S., Kleist, E., Mentel, T. F., Rohrer, F., Springer, M., Tillmann, R., Wildt, J., Wu, C., Zhao, D., Wahner, A., and Kiendler-Scharr, A.: Impact of NO<sub>x</sub> on secondary organic aerosol (SOA) formation from  $\alpha$ -pinene and  $\beta$ -pinene photooxidation: the role of highly oxygenated organic nitrates, *Atmos Chem Phys*, 20, 10125-10147, 10.5194/acp-20-10125-2020, 2020.
- 760 Quéféver, L. L. J., Kristensen, K., Normann Jensen, L., Rosati, B., Teiwes, R., Daellenbach, K. R., Peräkylä, O., Roldin, P., Bossi, R., Pedersen, H. B., Glasius, M., Bilde, M., and Ehn, M.: Effect of temperature on the formation of highly oxygenated



- organic molecules (HOMs) from alpha-pinene ozonolysis, *Atmos Chem Phys*, 19, 7609-7625, 10.5194/acp-19-7609-2019, 2019.
- 765 Rio, C., Flaud, P. M., Loison, J. C., and Villenave, E.: Experimental reevaluation of the importance of the abstraction channel in the reactions of monoterpenes with OH radicals, *Chemphyschem*, 11, 3962-3970, 10.1002/cphc.201000518, 2010.
- Rissanen, M. P., Kurtén, T., Sipilä, M., Thornton, J. A., Kangasluoma, J., Sarnela, N., Junninen, H., Jørgensen, S., Schallhart, S., Kajos, M. K., Taipale, R., Springer, M., Mentel, T. F., Ruuskanen, T., Petäjä, T., Worsnop, D. R., Kjaergaard, H. G., and 770 Ehn, M.: The formation of highly oxidized multifunctional products in the ozonolysis of cyclohexene, *J Am Chem Soc*, 136, 15596-15606, 10.1021/ja507146s, 2014.
- Rohrer, F., Bohn, B., Brauers, T., Brüning, D., Johnen, F. J., Wahner, A., and Kleffmann, J.: Characterisation of the photolytic HONO-source in the atmosphere simulation chamber SAPHIR, *Atmos Chem Phys*, 5, 2189-2201, 2005.
- 775 Romonosky, D. E., Laskin, A., Laskin, J., and Nizkorodov, S. A.: High-resolution mass spectrometry and molecular characterization of aqueous photochemistry products of common types of secondary organic aerosols, *J Phys Chem A*, 119, 2594-2606, 10.1021/jp509476r, 2015.
- Rossignol, S., Rio, C., Ustache, A., Fable, S., Nicolle, J., Mème, A., D'Anna, B., Nicolas, M., Leoz, E., and Chiappini, L.: The use of a housecleaning product in an indoor environment leading to oxygenated polar compounds and SOA formation: Gas and particulate phase chemical characterization, *Atmos Environ*, 75, 196-205, 10.1016/j.atmosenv.2013.03.045, 2013.
- 780 Saathoff, H., Naumann, K.-H., Möhler, O., Jonsson, Å. M., Hallquist, M., Kiendler-Scharr, A., Mentel, T. F., Tillmann, R., and Schurath, U.: A chamber study of secondary organic aerosol formation by limonene ozonolysis, *Atmos Chem Phys*, 9, 1551-1577, 2009.
- Shen, H., Vereecken, L., Kang, S., Pullinen, I., Fuchs, H., Zhao, D., and Mentel, T. F.: Unexpected significance of a minor reaction pathway in daytime formation of biogenic highly oxygenated organic compounds, *Sci Adv*, 8, 1-11, 2022.
- 785 Shen, H., Zhao, D., Pullinen, I., Kang, S., Vereecken, L., Fuchs, H., Acir, I. H., Tillmann, R., Rohrer, F., Wildt, J., Kiendler-Scharr, A., Wahner, A., and Mentel, T. F.: Highly Oxygenated Organic Nitrates Formed from NO<sub>3</sub> Radical-Initiated Oxidation of beta-Pinene, *Environ Sci Technol*, 55, 15658-15671, 10.1021/acs.est.1c03978, 2021.
- Taatjes, C. A.: Uncovering the Fundamental Chemistry of Alkyl+O<sub>2</sub> Reactions via Measurements of Product Formation, *J Phys Chem A*, 110, 4299-4312, 2006.
- 790 Tomaz, S., Wang, D., Zabalegui, N., Li, D., Lamkaddam, H., Bachmeier, F., Vogel, A., Monge, M. E., Perrier, S., Baltensperger, U., George, C., Rissanen, M., Ehn, M., El Haddad, I., and Riva, M.: Structures and reactivity of peroxy radicals and dimeric products revealed by online tandem mass spectrometry, *Nat Commun*, 12, 300, 10.1038/s41467-020-20532-2, 2021.
- Tröstl, J., Chuang, W. K., Gordon, H., Heinritzi, M., Yan, C., Molteni, U., Ahlm, L., Frege, C., Bianchi, F., Wagner, R., Simon, M., Lehtipalo, K., Williamson, C., Craven, J. S., Duplissy, J., Adamov, A., Almeida, J., Bernhammer, A. K., Breitenlechner, M., Brilke, S., Dias, A., Ehrhart, S., Flagan, R. C., Franchin, A., Fuchs, C., Guida, R., Gysel, M., Hansel, A., Hoyle, C. R., Jokinen, T., Junninen, H., Kangasluoma, J., Keskinen, H., Kim, J., Krapf, M., Kürten, A., Laaksonen, A., Lawler, M., Leiminger, M., Mathot, S., Möhler, O., Nieminen, T., Onnela, A., Petäjä, T., Piel, F. M., Miettinen, P., Rissanen, M. P., Rondo, L., Sarnela, N., Schobesberger, S., Sengupta, K., Sipilä, M., Smith, J. N., Steiner, G., Tomè, A., Virtanen, A., 800 Wagner, A. C., Weingartner, E., Wimmer, D., Winkler, P. M., Ye, P., Carslaw, K. S., Curtius, J., Dommen, J., Kirkby, J., Kulmala, M., Riipinen, I., Worsnop, D. R., Donahue, N. M., and Baltensperger, U.: The role of low-volatility organic compounds in initial particle growth in the atmosphere, *Nature*, 533, 527-531, 10.1038/nature18271, 2016.
- Valiev, R. R., Hasan, G., Salo, V. T., Kubečka, J., and Kurten, T.: Intersystem Crossings Drive Atmospheric Gas-Phase Dimer Formation, *J Phys Chem A*, 123, 6596-6604, 10.1021/acs.jpca.9b02559, 2019.
- 805 Vereecken, L. and Nozière, B.: H migration in peroxy radicals under atmospheric conditions, *Atmos Chem Phys*, 20, 7429-7458, 10.5194/acp-20-7429-2020, 2020.
- Vereecken, L. and Peeters, J.: Theoretical Study of the Formation of Acetone in the OH-Initiated Atmospheric Oxidation of  $\alpha$ -Pinene, *J Phys Chem A*, 104, 11140-11146, 2000.
- Vereecken, L. and Peeters, J.: The 1,5-H-shift in 1-butoxy\_ A case study in the rigorous implementation of transition state theory for a multirotamer system, *J Chem Phys*, 119, 5159-5170, 10.1063/1.1597479, 2003.
- 810 Vereecken, L. and Peeters, J.: Decomposition of substituted alkoxy radicals--part I: a generalized structure-activity relationship for reaction barrier heights, *Phys Chem Chem Phys*, 11, 9062-9074, 10.1039/b909712k, 2009.
- Vereecken, L. and Peeters, J.: A structure-activity relationship for the rate coefficient of H-migration in substituted alkoxy radicals, *Phys Chem Chem Phys*, 12, 12608-12620, 10.1039/c0cp00387e, 2010.
- 815 Vereecken, L. and Peeters, J.: A theoretical study of the OH-initiated gas-phase oxidation mechanism of beta-pinene (C<sub>10</sub>H<sub>16</sub>): first generation products, *Phys Chem Chem Phys*, 14, 3802-3815, 10.1039/c2cp23711c, 2012.
- Vereecken, L., Müller, J. F., and Peeters, J.: Low-volatility poly-oxygenates in the OH-initiated atmospheric oxidation of alpha-pinene: impact of non-traditional peroxy radical chemistry, *Phys Chem Chem Phys*, 9, 5241-5248, 10.1039/b708023a, 2007.
- 820 Vereecken, L., Vu, G., Wahner, A., Kiendler-Scharr, A., and Nguyen, H. M. T.: A structure activity relationship for ring closure reactions in unsaturated alkylperoxy radicals, *Phys Chem Chem Phys*, 23, 16564-16576, 10.1039/d1cp02758a, 2021.
- Waring, M. S.: Secondary organic aerosol formation by limonene ozonolysis: Parameterizing multi-generational chemistry in ozone- and residence time-limited indoor environments, *Atmos Environ*, 144, 79-86, 10.1016/j.atmosenv.2016.08.051, 2016.
- Williams, P. J. H., Boustead, G. A., Heard, D. E., Seakins, P. W., Rickard, A. R., and Chechik, V.: New Approach to the 825 Detection of Short-Lived Radical Intermediates, *J Am Chem Soc*, 144, 15969-15976, 10.1021/jacs.2c03618, 2022.



- Xu, L., Møller, K. H., Crounse, J. D., Otkjær, R. V., Kjaergaard, H. G., and Wennberg, P. O.: Unimolecular Reactions of Peroxy Radicals Formed in the Oxidation of alpha-Pinene and beta-Pinene by Hydroxyl Radicals, *J Phys Chem A*, 123, 1661-1674, 10.1021/acs.jpca.8b11726, 2019.
- 830 Yan, C., Nie, W., Äijälä, M., Rissanen, M. P., Canagaratna, M. R., Massoli, P., Junninen, H., Jokinen, T., Sarnela, N., Häme, S. A. K., Schobesberger, S., Canonaco, F., Yao, L., Prévôt, A. S. H., Petäjä, T., Kulmala, M., Sipilä, M., Worsnop, D. R., and Ehn, M.: Source characterization of highly oxidized multifunctional compounds in a boreal forest environment using positive matrix factorization, *Atmos Chem Phys*, 16, 12715-12731, 10.5194/acp-16-12715-2016, 2016.
- 835 Yan, C., Nie, W., Vogel, A. L., Dada, L., Lehtipalo, K., Stolzenburg, D., Wagner, R., Rissanen, M. P., Xiao, M., Ahonen, L., Fischer, L., Rose, C., Bianchi, F., Gordon, H., Simon, M., Heinritzi, M., Garmash, O., Roldin, P., Dias, A., Ye, P., Hofbauer, V., Amorim, A., Bauer, P. S., Bergen, A., Bernhammer, A. K., Breitenlechner, M., Brilke, S., Buchholz, A., Mazon, S. B., Canagaratna, M. R., Chen, X., Ding, A., Dommen, J., Draper, D. C., Duplissy, J., Frege, C., Heyn, C., Guida, R., Hakala, J., Heikkinen, L., Hoyle, C. R., Jokinen, T., Kangasluoma, J., Kirkby, J., Kontkanen, J., Kurten, A., Lawler, M. J., Mai, H., Mathot, S., Mauldin, R. L., Molteni, U., Nichman, L., Nieminen, T., Nowak, J., Ojdanic, A., Onnela, A., Pajunoja, A., Petaja, T., Piel, F., Quelever, L. L. J., Sarnela, N., Schallhart, S., Sengupta, K., Sipilä, M., Tome, A., Trostl, J., Vaisanen, O., 840 Wagner, A. C., Ylisirniö, A., Zha, Q., Baltensperger, U., Carslaw, K. S., Curtius, J., Flagan, R. C., Hansel, A., Riipinen, I., Smith, J. N., Virtanen, A., Winkler, P. M., Donahue, N. M., Kerminen, V. M., Kulmala, M., Ehn, M., and Worsnop, D. R.: Size-dependent influence of NO<sub>x</sub> on the growth rates of organic aerosol particles, *Sci Adv*, 6, ARTN eaay4945 10.1126/sciadv.aay4945, 2020.
- 845 Yu, J., Cocker III, D. R., Griffin, R. J., Flagan, R. C., and Seinfeld, J. H.: Gas-phase ozone oxidation of monoterpenes: Gaseous and particulate products, *J Atmos Chem*, 34, 207-258, Doi 10.1023/A:1006254930583, 1999.
- Zhang, H., Yee, L. D., Lee, B. H., Curtis, M. P., Worton, D. R., Isaacman-VanWertz, G., Offenberg, J. H., Lewandowski, M., Kleindienst, T. E., Beaver, M. R., Holder, A. L., Lonneman, W. A., Docherty, K. S., Jaoui, M., Pye, H. O. T., Hu, W., Day, D. A., Campuzano-Jost, P., Jimenez, J. L., Guo, H., Weber, R. J., de Gouw, J., Koss, A. R., Edgerton, E. S., Brune, W., Mohr, C., Lopez-Hilfiker, F. D., Lutz, A., Kreisberg, N. M., Spielman, S. R., Hering, S. V., Wilson, K. R., Thornton, J. A., 850 and Goldstein, A. H.: Monoterpenes are the largest source of summertime organic aerosol in the southeastern United States, *Proc Natl Acad Sci U S A*, 115, 2038-2043, 10.1073/pnas.1717513115, 2018.
- Zhao, D., Pullinen, I., Fuchs, H., Schrade, S., Wu, R., Acir, I.-H., Tillmann, R., Rohrer, F., Wildt, J., Guo, Y., Kiendler-Scharr, A., Wahner, A., Kang, S., Vereecken, L., and Mentel, T. F.: Highly oxygenated organic molecule (HOM) formation in the isoprene oxidation by NO<sub>3</sub> radical, *Atmos Chem Phys*, 21, 9681-9704, 10.5194/acp-21-9681-2021, 2021.
- 855 Zhao, D., Schmitt, S. H., Wang, M., Acir, I.-H., Tillmann, R., Tan, Z., Novelli, A., Fuchs, H., Pullinen, I., Wegener, R., Rohrer, F., Wildt, J., Kiendler-Scharr, A., Wahner, A., and Mentel, T. F.: Effects of NO<sub>x</sub> and SO<sub>2</sub> on the secondary organic aerosol formation from photooxidation of  $\alpha$ -pinene and limonene, *Atmos Chem Phys*, 18, 1611-1628, 10.5194/acp-18-1611-2018, 2018.
- 860 Zhao, D. F., Buchholz, A., Kortner, B., Schlag, P., Rubach, F., Kiendler-Scharr, A., Tillmann, R., Wahner, A., Flores, J. M., Rudich, Y., Watne, Å. K., Hallquist, M., Wildt, J., and Mentel, T. F.: Size-dependent hygroscopicity parameter ( $\kappa$ ) and chemical composition of secondary organic cloud condensation nuclei, *Geophys Res Lett*, 42, 10,920-910,928, 10.1002/2015gl066497, 2015a.
- Zhao, D. F., Kaminski, M., Schlag, P., Fuchs, H., Acir, I. H., Bohn, B., Häseler, R., Kiendler-Scharr, A., Rohrer, F., Tillmann, R., Wang, M. J., Wegener, R., Wildt, J., Wahner, A., and Mentel, T. F.: Secondary organic aerosol formation from hydroxyl radical oxidation and ozonolysis of monoterpenes, *Atmos Chem Phys*, 15, 991-1012, 10.5194/acp-15-991-2015, 2015b.
- 865 Zhao, Y. and Truhlar, D. G.: The M06 suite of density functionals for main group thermochemistry, thermochemical kinetics, noncovalent interactions, excited states, and transition elements: two new functionals and systematic testing of four M06-class functionals and 12 other functionals, *Theor Chem Account*, 120, 215-241, 10.1007/s00214-007-0310-x, 2008.
- 870 Ziemann, P. J. and Atkinson, R.: Kinetics, products, and mechanisms of secondary organic aerosol formation, *Chem Soc Rev*, 41, 6582-6605, 10.1039/c2cs35122f, 2012.